isvr Institute of Sound and Vibration Research

Feedback Control of the Sound Inwardly Radiated by an Aircraft Panel Excited by a Turbulent Boundary Layer

P. Augereau

ISVR Technical Memorandum 869

August 2001

University of Southampton

SCIENTIFIC PUBLICATIONS BY THE ISVR

Technical Reports are published to promote timely dissemination of research results by ISVR personnel. This medium permits more detailed presentation than is usually acceptable for scientific journals. Responsibility for both the content and any opinions expressed rests entirely with the author(s).

Technical Memoranda are produced to enable the early or preliminary release of information by ISVR personnel where such release is deemed to the appropriate. Information contained in these memoranda may be incomplete, or form part of a continuing programme; this should be borne in mind when using or quoting from these documents.

Contract Reports are produced to record the results of scientific work carried out for sponsors, under contract. The ISVR treats these reports as confidential to sponsors and does not make them available for general circulation. Individual sponsors may, however, authorize subsequent release of the material.

UNIVERSITY OF SOUTHAMPTON

INSTITUTE OF SOUND AND VIBRATION RESEARCH

SIGNAL PROCESSING & CONTROL GROUP

Feedback Control of the Sound Inwardly Radiated by an Aircraft Panel Excited by a Turbulent Boundary Layer

by

P Augereau

ISVR Technical Memorandum No. 869

August 2001

Authorised for issue by
Prof S J Elliott
Group Chairman

Acknowledgements

The work presented in this report has been completed at the Institute of Sound and Vibration Research. I would thank all the members of this laboratory for their help and welcome.

I would particularly thank Professor S. Elliott and Dr. C. Maury, without whom this stay would not have been possible.

Contents

Part C- Results

Introduction

Norms against the noise and vibration pollution are more and more strict. In the aeronautical domain, since the sound radiated by the jet engines and propellers has been significantly reduced, aircraft manufacturers are now interested in reducing the sound and vibrations generated, under cruise conditions, in the cabin by the airflow developed over the fuselage. Thus, the studies on the active control of the turbulent boundary layer (TBL) induced noise in aircraft cabin become an interesting axis of research in acoustics since a few years. Unfortunately, there is not a lot of experiment in this field. The aim of this internship is to build and validate a reliable model for the feedback control of the sound power inwardly radiated by an aircraft panel excited by a TBL, by comparison with measurements results recently obtained by G. Gibbs at the NASA Langley Research Center. If the model is representative, it could then be used in conjonction with a model for the acoustic response of an aircraft cabin enclosure.

As many laboratories do not have an anechoic wind tunnel to achieve this kind of experiments (due to the cost of such installations), there is also a need to simulate the sound radiated by a structure excited by a TBL, and the present study could also be used to show the feasibility of TBL simulations in laboratory.

This report is organised as follows. Part A presents the theoretical simulation of the problem. It introduces the models for the TBL excitation and the panel vibro-acoustic response as well as the theory of feedback control systems used to suppress random disturbances. The second part of this report, part B, exposes the way used to simulate different control strategy, their implementation and their results. In particular, the G. Gibbs feedback control experiments about the reduction of flow-induced noise will be exposed. The last part is the conclusion.

Part A: Theoretical study of the problem

Before to investigate the control of the sound radiated by an airplane, the basic problem of a plate should be understood. It is necessary to study the reaction of a panel to an excitation. This study is only concerned with a vibrating panel. A full aircraft model would be an extension of this work. This part presents the models for the TBL excitation, the plate and the panel vibro-acoustic response. Finaly, a introduction to the feedback control is presented.

A-1. Model for the turbulent boundary layer excitation

In order to realise some experiments on aircraft structure under cruise conditions while, in the meantime, avoiding the cost and disadvantages of a real experiment, there is a need to build a representative model in order to describe the acoustic and structural response of an aircraft panel. For most of the models that have been developed (ref [1]), use has been made of the following assumptions.

First, it is usually assumed that the surface pressure fluctuations are not modified by the vibrations of the flexible plate (ref [2]). Thus, the pressure developed on the structure is the pressure that would be observed on a rigid structure, also called the blocked pressure p_b.

Second, it is assumed that the TBL is fully developed when exciting the plate. It means that the turbulent wall-pressure field is homogeneous in time and space. The wall-pressure field of interest is far enough from the front edge of an aircraft (under cruise conditions) for this hypothesis to be valid (ref [3]).

Third, for the acoustic wave propagation within the external flow, the fluid is considered to be at rest. This hypothesis will not affect the sound pressure field inwardly radiated by the plate, because this sound pressure field is not significantly affected by the fluid flow above the plate, at least for subsonic flows. Indeed, the acoustic fluid load mainly depends on the mechanical properties of the fluid in the immediate neighbourhood of the plate, where the fluid flow velocity is close to zero (ref [4]).

Finally, it is noticed that this study is concerned with the sound radiated by a panel in an anechoic enclosure. The structural-acoustic coupling with the resonances of the cabin enclosure are not considered in a first step. Only the low-frequency domain is concerned by this assumption. It will have to be considered in future researches.

The system studied is sketched in Figure 1.

An empirical model for the wall-pressure distribution due to a TBL is the one proposed by Corcos in 1964 (ref [5,6]). We keep in mind that this model is only valid for a random pressure field stationary in time and homogeneous in space, which is the case for a TBL developed over the fuselage of an aircraft under cruise conditions. Corcos suggested that the cross spectral density between the pressures measured between two points A and B at an angular frequency ω has the form:

$$S_{p_b p_b}(\xi_x, \xi_y, \omega) = \phi_0(\omega) e^{-\alpha_x |\omega \xi_x / U_c|} e^{-\alpha_y |\omega \xi_y / U_c|} e^{-j\omega \xi_y / U_c}, \qquad (1)$$

where:

$\phi_0(\omega)$ is the power spectral density of the wall-pressure fluctuations. In this study this function is chosen to be equal to the one proposed by Efimtsov (ref [7]) which is valid up to high subsonic Mach numbers (ref [2]). This model is given as a function of the Strouhal number $Sh = \omega\delta / U_\infty$ by:

$$\phi_0(\omega) = \frac{\tau_\omega^2 \delta}{U_\tau} \frac{0.01\pi}{(1+0.02Sh^{2/3})}, \quad U_\tau = \sqrt{\frac{\tau_\omega}{\rho_+}} \quad , \tag{2}$$

where δ is the boundary layer thickness, τ_ω is the mean wall shear stress, and U_τ is the friction velocity.

$\xi_x = x - x'$ and $\xi_y = y - y'$ denote respectively the spanwise and the streamwise separation distances.

U_c is the eddy convection velocity.

α_x and α_y are constants derived from experiments. In this study, this constants are assumed to be respectively 0.7 and 0.1.

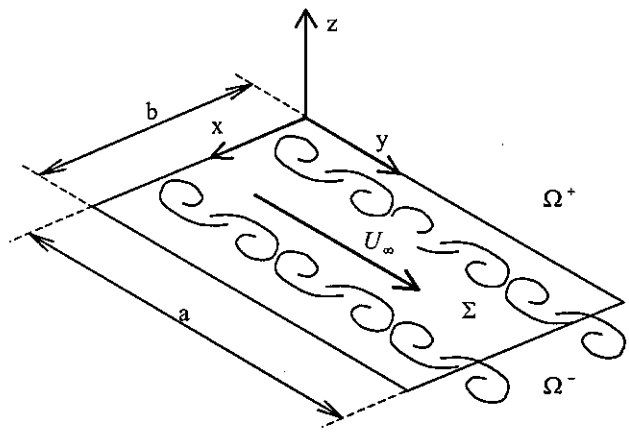

Figure 1: A flat panel excited on one side by a turbulent airflow with the free-stream velocity U_∞.

The streamwise direction is the y-direction and the spanwise direction is the x-direction. The wall pressure fluctuations due to the TBL induce the vibration of the panel that radiates acoustic energy in both fluid domains from each side of the plate.

From equation (1), it can be seen that the cross spectral density between two points falls off more quickly as the points are separated in the spanwise direction than in the streamwise direction, and that there is a phase shift between the pressures only in the streamwise direction due to the convection velocity. It can also be remarked that in the time domain, the cross-correlation function of the pressure field between points separated by a distance x exhibits a maximum after a delay $\tau = x / U_c$, which corresponds to the time taken to transport the perturbation a distance x streamwise, with the convection velocity U_c (ref [8]).

The Corcos spectrum of the excitation is sufficient for this study because it can be shown (ref [4]) that it provides a good estimation for the wall-pressure fluctuation levels at and near the convective peak in the wavenumber domain representation, which is of fundamental importance for aircraft boundary layers.

A-2. The aircraft panel model

With the Corcos model, the statistical properties of the TBL pressure field observed on an aircraft fuselage can be calculated, but there is also a need to model the fuselage dynamics. As a first step, only one panel of the aircraft fuselage is considered, assuming that it radiates sound pressure independently from the adjacent panels. Such a model has been confirmed as representative by extensive flight test measurements for frequencies above 400 Hertz (ref [9]). In the low frequency domain (in the sense of low modal density), it would be better to account for flexible lateral reinforcements between each panel. This is actually under study because of the main importance of the low frequencies in an active control approach.

Further approximations are used to model the structure (ref [4,10]). The adjacent bays of an aircraft fuselage are set in a cylindrical shell and the effects of curvature have their importance. Indeed, a study has shown that the curvature effects modifies the noise radiated inside the aircraft cabin (ref [11]). One way to neglect it would be to fill an aircraft cabin with a material sufficiently hard, to appear as a baffle, and in the meantime sufficiently absorbing, to neglect the returned sound waves. Such conditions are hardly met in aircraft cabins. Thus, the curvature effect seems difficult to be neglected. Fortunately, the curvature is not the only effect that influences the panel response. In practice, the influence of curvature still appears to be negligible when compared with the influence of in-plane stresses acting on the boundaries of the panel (ref [4]).

Indeed, as there is a pressure difference between the exterior and the interior of the fuselage structure, as a consequence of the cabin pressurisation under cruise conditions, membrane tensions have to be modelled. It has been shown that these tensions lead to an increase of the fundamental resonance frequency of each panel by a factor of up to about 7 (ref [10]).

Hence, the main physical characteristics of the problem are retained by considering the simplified but relevant model of a simply supported flat plate stressed by tension forces. It is better to consider the panel to be simply supported on its boundaries than to be clamped into a rigid wall. In fact, this hypothesis provides a model in better agreement with *in situ* vibrations measurements.

Finally, some hypothesis have to be added to this simplified model. First, the plate material is considered to be homogeneous and isotropic. Then, it is assumed that the fluids on each side are perfect. Finally, the panel structural damping is modelled: an equivalent damping coefficient ξ is introduced, the damping ratio. This coefficient is representative of two kinds of damping: the internal or *hysteretic* damping and the boundary damping due to the frictions in the joint edges or due to the energy lost by the panel through its elastic boundaries. It can be shown that in our configuration the second effect is much more important than the first one (ref [2]).

At this stage, a model of an aircraft panel has been defined. The simulation of the problem is then possible, so a study to predict and reduce the sound power radiated inside the cabin of an aircraft can be lead.

A-3. Formulation of the vibro-acoustic problem

Before investigating the active control of the noise induced by a TBL excitation, the physics of the problem has to be understood.

In order to predict the acoustic field radiated in the cabin by an aircraft panel, the structural displacement has to be known. The TBL developed over an aircraft panel generates wall-pressure fluctuations, that are described by a stochastic field, p_b, which is stationary up to order 2 in time and space. These pressure fluctuations excite the panel and induce a normal displacement w. Finally, the plate radiates in both fluid domains. It can be shown that this displacement is also a stochastic field, which is stationary up to order 2 with respect to the time, but not stationary with respect to the space.

A-3-a- Derivations of the expressions for the power spectral densities of the panel velocity and sound pressure radiated

The basic of the problem is the vibration of a plate which induce sound radiation in the fluid above and below it. Due to this fact, the main characteristics will be deduce from the basic system of equation verified by the displacement w of the panel and the pressure fields $p^{\pm}(\mathbf{x};t)$ in the fluid, and the limits equations (3):

$$
\begin{cases}
\left(D'\Delta_x^2 + N_x'\frac{\partial^2}{\partial x^2} + N_y'\frac{\partial^2}{\partial y^2} - m\frac{\partial^2}{\partial t^2} \right) w(\mathbf{x},t) = -p_b(\mathbf{x};t) - \lim_{z\to 0^+}[p^+(\mathbf{x};t) - p^-(\mathbf{x};t)], \ \forall \mathbf{x}\in\Sigma, \\
(\Delta - \frac{1}{c_{\pm}^2}\frac{\partial^2}{\partial t^2})p^{\pm}(\mathbf{z};t) = 0, \quad \forall \mathbf{z}\in\Omega^{\pm}, \\
\rho_{\pm}\frac{\partial^2 w}{\partial t^2}(\mathbf{x};t) + \frac{\partial p^{\pm}}{\partial z}(\mathbf{x};t) = 0, \quad \forall \mathbf{x}\in\Sigma, \\
\frac{\partial p^{\pm}}{\partial z}(\mathbf{x};t) = 0, \quad \forall \mathbf{x}\in\Sigma, \\
\textit{Boundary conditions for } w \textit{ onto } \partial\Sigma, \\
\textit{Sommerfeld radiation conditions for } p^+ \textit{ and } p^-, \\
\textit{Initial conditions for } w,\ p^+ \textit{ and } p^-.
\end{cases}
\tag{3}
$$

It would be convenient to apply a time-Fourier transform to this system in order to solve it. Unfortunately, the excitation term $p_b(\mathbf{x};t)$ is random, so it does not possess a time-Fourier transform. Then, the strategy is to use a Green formulation (ref [4]) to express the panel displacement. The Green's kernel of the motion of the fluid-

loaded plate, $\gamma(\mathbf{x}-\mathbf{x}';\omega)$, is defined as the solution of the problem when the random excitation, $p_b(\mathbf{x};t)$, is replaced by the harmonic point force excitation $\delta_{\mathbf{x}'}(\mathbf{x})e^{i\omega t}$. Thus, the displacement of the plate can be represented using an integral representation:

$$w(\mathbf{x},t) = (\gamma * p_b)(\mathbf{x},t) = \int_{-\infty}^{+\infty}\iint_{R^2}\gamma(\mathbf{x}-\mathbf{x}';t-\tau)p_b(\mathbf{x}';\tau)d\tau\ d\mathbf{x}', \forall \mathbf{x}\in\Sigma, \forall t, \quad (4)$$

where * denotes a convolution product with respect to the inverse Fourier transform $\gamma(\mathbf{x};t)$ of $\gamma(\mathbf{x}-\mathbf{x}';\omega)$ with respect to frequency.
The calculation of the power spectral density of the panel velocity leads to the following expression (ref [4]):

$$S_{ww}(\mathbf{x},\mathbf{x}',\omega) = \frac{1}{(2\pi)^2}\int_{-\infty-\infty}^{+\infty+\infty}\Gamma_\omega(\mathbf{x};\mathbf{k})S_{p_bp_b}(\mathbf{k};\omega)\Gamma_\omega^*(\mathbf{x}';\mathbf{k})d^2\mathbf{k}\ , \quad (5)$$

where the superscript * denotes the conjugate of a complex number. $\Gamma_\omega(\mathbf{x};\mathbf{k})$ is the displacement of a point at a position $\mathbf{x}$ on the fluid loaded plate, calculated at the angular frequency ω and when the excitation pressure p_b scales on the contribution of a boundary layer eddy of wavevector $\mathbf{k}$:

$$\Gamma_\omega(\mathbf{x},\mathbf{k}) = \iint_\Sigma \gamma(\mathbf{x}-\mathbf{x}';\omega)e^{-j\mathbf{k}.\mathbf{x}'}d^2\mathbf{x}', \forall \mathbf{k}\in R^2, \forall\omega\ . \quad (6)$$

From equation (5), it is relevant to note that the displacement induced by the TBL excitation on the plate can be seen as the result of the excitation $S_{p_bp_b}$ passing through a linear filter characterized by the transfer function Γ_ω. So the plate can be interprated as a wavevector filter of the excitation spectrum.

By definition, $\Gamma_\omega(\mathbf{x},\mathbf{k})$ satisfies the following system of equation (ref [4]):

$$\begin{cases} (D'\Delta_x^2 + N_x'\dfrac{\partial^2}{\partial x^2} + N_y'\dfrac{\partial^2}{\partial y^2} - m\omega^2)\Gamma_\omega(\mathbf{x},\mathbf{k}) = -e^{-j\mathbf{k}.\mathbf{x}} - [p_\omega^+(\mathbf{x};\mathbf{k}) - p_\omega^-(\mathbf{x};\mathbf{k})], \forall \mathbf{x}\in\Sigma, \\ (\Delta + \underset{-}{k}_+^2)p_\omega^+(\mathbf{z};\mathbf{k}) = 0, \quad \forall \mathbf{z}\in\Omega^+, \\ \dfrac{\partial p_\omega^+}{\partial z}(\mathbf{x};\mathbf{k}) = \underset{-}{\rho}_+\omega^2\Gamma_\omega(\mathbf{x};\mathbf{k}), \quad \forall \mathbf{x}\in\Sigma, \\ \dfrac{\partial p_\omega^+}{\partial z}(\mathbf{x};\mathbf{k}) = 0, \quad \forall \mathbf{k}\in\Sigma, \\ \textit{Boundary conditions for } \Gamma_\omega(\mathbf{x},\mathbf{k}) \textit{ when } \mathbf{x}\in\partial\Sigma', \\ \textit{Sommerfeld radiation conditions for } p_\omega^+ \textit{ and } p_\omega^-. \end{cases} \quad (7)$$

All the structural quantities are defined over the mean surface Σ $(z=0)$ of the panel. The boundary of the panel is denoted $\partial\Sigma$ and its complement in the $(z=0)$ plan is

defined as being a perfectly rigid baffle: Σ'. $D = Eh^3/12(1-\nu^2)$ is the bending stiffness of the plate. m is the mass density of the plate. E and ν are respectively the Young's modulus of elasticity and the Poisson's ratio of the plate material. N_x' and N_y' are the lateral and longitudinal tension terms acting on the panel and due to the cabin pressurisation. The pressure field inwardly radiated by the panel is denoted p_ω^-.

The power spectral density $S_{p^-p^-}(z,z';\omega)$ of the acoustic pressure field radiated in the fluid domain Ω^- is given by:

$$S_{p^-p^-}(\mathbf{z},\mathbf{z}';\omega) = \frac{1}{(2\pi)^2}\int_{-\infty-\infty}^{+\infty+\infty}\int p_\omega^-(\mathbf{z};\mathbf{k})S_{p_bp_b}(\mathbf{k};\omega)p_\omega^{-*}(\mathbf{z}';\mathbf{k})d^2\mathbf{k}, \forall(\mathbf{z},\mathbf{z}')\in\Omega^-, \forall\omega\,. \quad (8)$$

The sound pressure field $p_\omega^-(\mathbf{x};\mathbf{k})$ can be calculated by using its Green's representation. Thus, p_ω^- takes the integral form:

$$p_\omega^-(\mathbf{z};\mathbf{k}) = \rho_-\omega^2\iint_\Sigma G_\omega^-(\mathbf{z}-\mathbf{x}')\Gamma_\omega(\mathbf{x}';\mathbf{k})d^2\mathbf{x}', \quad \forall\,\mathbf{z}\in\Omega^-, \forall\,\mathbf{k}\in R^2, \quad (9)$$

where G_ω^- is the Green's function of the Helmholtz equation for acoustic propagation in the half space Ω^-, which satisfies the homogeneous Neumann boundary condition on $(z=0)$ as well as the Sommerfeld conditions at infinity. It is given by:

$$G_\omega^-(\mathbf{z}-\mathbf{z}') = \frac{e^{-jk\_r(\mathbf{z},\mathbf{z}')}}{4\pi r(\mathbf{z},\mathbf{z}')} + \frac{e^{-jk\_r(\mathbf{z},\mathbf{z}\_')}}{4\pi r(\mathbf{z},\mathbf{z}\_')}, \forall(\mathbf{z},\mathbf{z}')\in\Omega^-\times\Omega^-, \quad (10)$$

where $\mathbf{z}'$ is the symmetric point of $\mathbf{z}$ with respect to the plate plane, and $r(\mathbf{z},\mathbf{z}')$ denotes the distance between $\mathbf{z}$ and $\mathbf{z}'$.

A-3-b- Derivations of the expressions for the plate kinetic energy and for the sound power radiated

At this stage, $\Gamma_\omega(\mathbf{x};\mathbf{k})$ has to be calculated for each wavenumber $\mathbf{k}$ to solve the problem. This can be achieved using an eigenmode decomposition of the panel structural response, as it is shown below.

The derivative of the displacement $\Gamma_\omega(\mathbf{x};\mathbf{k})$ with respect to the spatial variable will be considered: it represents the velocity $v_\omega(x,y,0;\mathbf{k})$ of the plate.

In a first step, the velocity is specified in terms of the amplitudes v_{mn} of an infinite set of eigenmodes or structural modes of the plate such as:

$$v_\omega(x,y,0,\mathbf{k}) = j\omega\sum_{m=1}^{+\infty}\sum_{n=1}^{+\infty}v_{mn}(\mathbf{k};\omega)W_{mn}(x,y)\,. \quad (11)$$

Introducing this expression in the equation system (7), the plate velocity is obtained as:

$$v_\omega(x,y,0;\mathbf{k}) = j\omega\sum_{m=1}^{+\infty}\sum_{n=1}^{+\infty} F_{mn}(\mathbf{k})a_{mn}(\omega)W_{mn}(x,y), \tag{12}$$

where W_{mn} represent the eigenmodes of the plate, F_{mn} the modal excitation terms and a_{mn} the modal resonance terms.

For a simply supported panel of dimensions a and b, the eigenmodes and eigenfrequencies are given by:

$$W_{mn}(x,y) = \frac{2}{\sqrt{ab}}\sin(\frac{m\pi x}{b})\sin(\frac{n\pi y}{a}) \ , \tag{13}$$

$$\omega_{mn}^2 = \frac{1}{\rho h}(\frac{Eh^3}{12(1-\nu^2)}[(\frac{m\pi}{b})^2 + (\frac{n\pi}{a})^2]^2 + N_x(\frac{m\pi}{b})^2 + N_y(\frac{n\pi}{a})^2) \ . \tag{14}$$

The modal excitation terms are defined as follows:

$$F_{mn}(\mathbf{k}) = \int_\Sigma W_{mn}(\mathbf{x})e^{-j\,\mathbf{k}.\mathbf{x}}d^2\mathbf{x} \quad . \tag{15}$$

Each of these terms represents the influence on each structural mode of a turbulent eddy scaled on each wavenumber **k**.
The modal resonance terms are given by:

$$a_{mn}(\omega) = \frac{1}{\rho_p h[\omega_{mn}^2 - \omega^2 + 2j\xi\omega_{mn}\omega]} \quad , \tag{16}$$

where $m = \rho_p h$. After inserting equations (12)-(16) into equation (5), the power spectral density of the panel displacement can be written as (ref [4]):

$$S_{ww}(\mathbf{x},\mathbf{x}';\omega) = \frac{1}{(2\pi)^2}\sum_{m=1}^{+\infty}\sum_{n=1}^{+\infty}\sum_{p=1}^{+\infty}\sum_{q=1}^{+\infty}\psi_{\{m,n,p,q\}}(\omega)W_{mn}(\mathbf{x})W_{pq}^*(\mathbf{x}')a_{mn}(\omega)a_{pq}^*(\omega), \quad \forall(\mathbf{x},\mathbf{x}') \in \Sigma\times\Sigma \tag{17}$$

A matrix of modal excitation terms ψ appears and is defined by:

$$\psi_{\{i,j,k,l\}}(\omega) = 4\pi^2\int_{-\infty}^{+\infty}\int_{-\infty}^{+\infty} F_{ij}(\mathbf{k})S_{pp}(\mathbf{k};\omega)F_{kl}^*(\mathbf{k})d\mathbf{k}, \tag{18}$$

where each coefficient quantifies how the structural modes are coupled by the turbulent excitation. An expression of the spectral density S_V of the kinetic energy in the structure can be deduced together with the spectral density of the sound power S_π inwardly radiated by the plate (ref [10]). If the modal resonance terms are stored in a diagonal matrix, denoted $D_\omega(a)$, these expressions are respectively given, in matrix notations, as:

$$S_V(\omega) = \frac{\rho_p h \omega^2}{2} Tr[D_\omega^H(a)\psi_\omega D_\omega(a)], \tag{19}$$

and

$$S_{\pi^-}(\omega) = \frac{\omega \rho_- c_-}{2} Tr[D_\omega^H(a)\Re(M_\omega^-)D_\omega(a)\psi_\omega], \tag{20}$$

where M_ω^- is defined as the radiation impedance matrix:

$$M^-_{\omega,(i,j,k,l)} = \langle P_{ij}^-(\mathbf{x};\omega), W_{kl}^*(\mathbf{x})\rangle_\Sigma, \tag{21}$$

and $P_{ij}^-(M) = \int_\Sigma W_{ij}(M') \frac{e^{-i\mathbf{k}_0 d(M,M')}}{4\pi d(M,M')} d\Sigma(M')$. It represents the acoustic field inwardly radiated by the ij^{th} structural mode. $\langle \mathbf{u}, \mathbf{v}\rangle_\Sigma = \int_\Sigma (\mathbf{u}\mathbf{v}^*)(M) d\Sigma(M)$ for any test functions $\mathbf{u}$ and $\mathbf{v}$.

The fact that the cross-terms of the M_ω^- matrix in (20) are not zero-valued means that the pressure fields inwardly radiated by two different modes are coupled. Thus, if the contribution of two different structural modes are coupled, suppressing the influence of one structural mode may not reduce the total sound power radiated. Fortunately, it is possible to express the M_ω^- matrix in a new basis, where it has a diagonal form.

A-3-c- Expression of the problem in the radiation modes formulation

Here, it can be stressed that the final aim is not to reduce overall vibration levels, but to alter the vibrations in such a way that the total sound power radiated is reduced.This is also called an active structural acoustic control (ASAC). Sometimes, it can be achieved even though the overall kinetic energy of the plate is increased. This has been shown in some studies like in references [10,12,13]. It has also been shown in these studies, performed with an harmonic excitation, that cancelling the radiation modes provides better results than cancelling the structural modes.

To this aim, the authors of references [14,4] have computed the radiation modes of a simply-supported baffled plate, which are a basis of source distributions which contribute orthogonally to the sound power radiated. Hence, it is sure that suppressing the radiation modes of each aircraft panel will reduce the sound power inwardly radiated by the fuselage into the cabin. It should be noted that these radiation modes are dependent of the frequency. In practice, it is possible to pass over the problem of sensing the frequency dependence of the radiation modes by using their nesting property, i.e. to sense a set of radiation modes at a fixed upper frequency (ref [15]).

Here, the case of a plate divided in an array of I small elements is studied. So the panel is viewed as a sum of elemental radiators, acting individually like pistons. Then, the sound pressure inwardly radiated by the plate will be calculated from the contribution of each one of these elemental sources. For the simplicity of the

equations, a harmonic excitation is considered, but the method is exactly the same for a TBL excitation. The deterministic sound power radiated, W, is then replaced by its spectral density, S_p.

Let us denote v the vector of complex linear velocities of each of the elemental radiators at a single, W can be written under a harmonic excitation (ref [14]) as:

$$W = \mathbf{v}^H \mathbf{R} \mathbf{v}, \tag{22}$$

where R is the discretized form of the radiation resistance matrix $\Re[M_\omega^-]$. It has been shown that R is a purely real, symmetric and positive definite matrix. Thus, its eigenvalue-eigenvector decomposition can be expressed as follows:

$$\mathbf{R} = \mathbf{Q}^T \Lambda \mathbf{Q}, \tag{23}$$

where $\mathbf{Q}$ is the orthogonal matrix of the eigenvectors and Λ is the diagonal matrix of the eigenvalues λ_i.

Hence, if the vector of radiation modes in terms of the velocities of each individual elements is defined as $\mathbf{y}$, the equations (22) and (23) give the following expression for the sound power radiated by the panel:

$$W = \mathbf{y}^H \Lambda \mathbf{y} = \sum_{i=1}^{I} \lambda_i |y_i|^2 . \tag{24}$$

In this expression it can be seen that the radiation modes radiate sound independently from each others.

Now it is understood that if the different radiation modes of an aircraft panel are known, it will be possible to reduce the total sound pressure field radiated, reducing the contribution of one or more radiation modes. In fact, it can be shown that for the low frequencies (below 40 Hertz for a panel without tension effects, and below 400 Hertz for a panel submitted to tension effects), the first radiation mode, which acts like a piston, is responsible for almost the whole sound power radiated. Due to this fact, reducing only the first radiation mode will provide a good reduction of the sound power radiated by the panel.

However, it is not so convenient to use the radiation modes because they have to be calculated for each frequency of interest. For a TBL excitation, the disturbing noise is broadband and these modes have to be calculated several times. Fortunately, it can be shown that it is a good approximation to consider only the radiation modes obtained for the upper frequency of the bandwidth of interest (ref [15]). This is achieved using the RME technique developed by G.Gibbs *et al.*. This method will not be presented there, but for more information, the reference 15 can be consulted.

Now, the active control method can be applied to reduce the velocity of the first radiation mode in order to reduce the total sound pressure field inwardly radiated by an aircraft fuselage.

A-3-d- Summary of the method

As a summary of this part, a diagram of the problem can be drawn. This permits to establish a parallel between two main way to achieve the cancellation of the sound power radiated by a panel. The first one is to suppress the contribute of each structural mode (like in reference 16) and the second one is to suppress the contribution of the radiation modes.

In each case, the minimum number of modes required to have a good approximation of the acoustic power radiated is researched. The studies have also shown that cancelling higher order radiation modes is the most efficient strategy. For example, in the configuration considered in reference [4], when 3 of these modes are suppressed, it provides the same level of attenuation than cancelling 6 structural modes (ref [10]). This is the reason why it is more interesting to suppress the radiation modes.

The problem diagram is the following one:

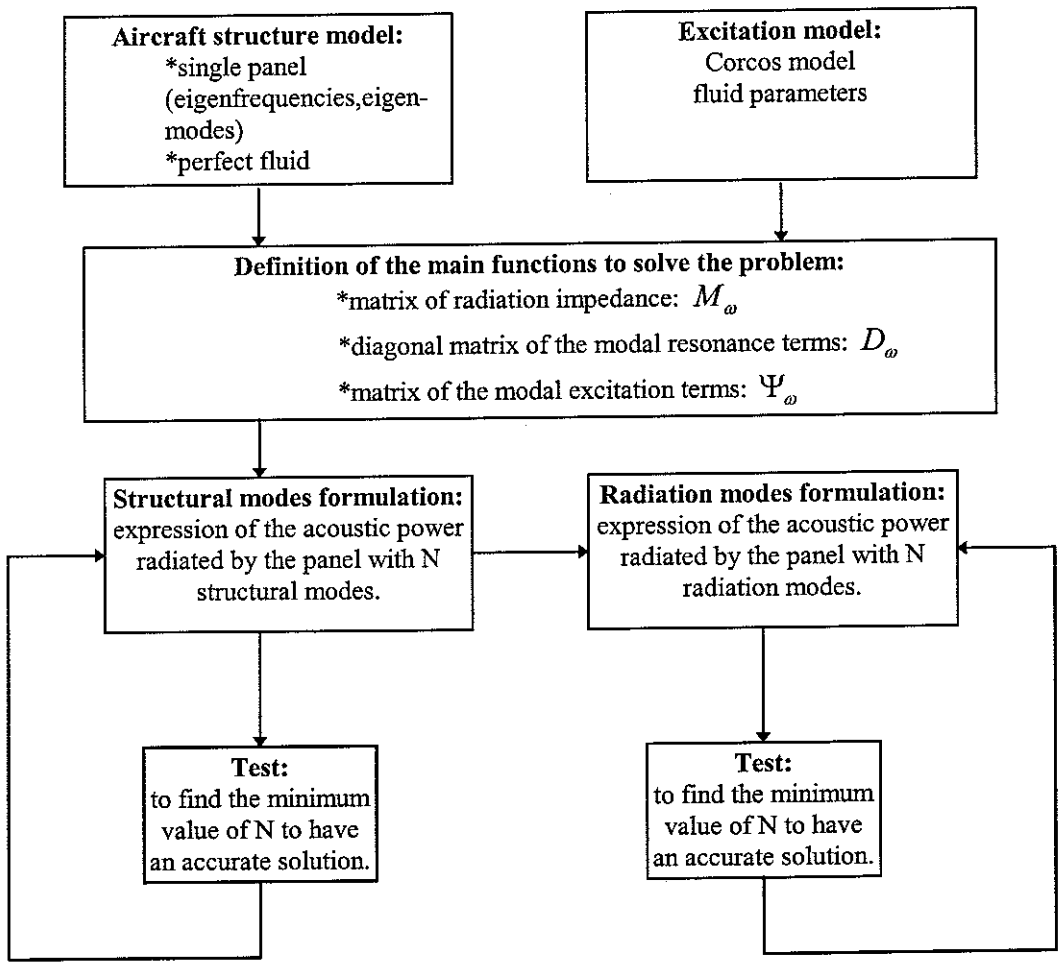

Figure 2: Synoptic diagram of the resolution method with the structural/radiation modes approaches

A-4. Principle of the feedback control

Now, an active structural acoustic control approach (ASAC) can be studied. This kind of control is well described in the references 12 and 17. The main idea is presented below.

In this study, the disturbing noise is random. For such noises, the main problem is that there is no time-advanced reference signals that can be observed and so a feedforward active control is not possible. In fact some studies presented a feedforward control for such noise sources (ref [18,13]) using, as a reference, the signal from an accelerometer, which is assumed to be independent of the error signal, but such studies were realized in a laboratory, and it is not so convenient to implement such a control on a real aircraft. Therefore, a feedback control strategy is prefered as it does not require any reference signal.

First of all, it can be noticed that the spectrum of a TBL-induced noise, as measured in reference 3, is situated in a frequency range where an active control is possible. In fact, the dominating part of this spectrum is around 1000 Hertz, where the noise radiated can be well represented by only the influence of the first few radiation or structural modes. Thus, an active control device acting on a limited number of modes can be implemented.

Second, it can be stressed that the three elementary components of feedback control system are a sensor, to detect the vibrations of the panel, an electronic controller, to compensate for the disturbance, and an actuator, driven by the output signal from the controller. More details about the sensors and the actuators used in this study can be found in references 19 to 22. However, these elements will not be described, but they have to be considered since they modify the plant system transfer function.

As a first step, a feedback control of vibration with only one sensor and one actuator (ref 12 & 23) will be considered. The basic idea is to sense both the vibration of the plate, induced by the primary source, and the vibration induced by the secondary actuator, and to feed back the control signal, obtained by passing the sensor output through the control filter, to the actuator.

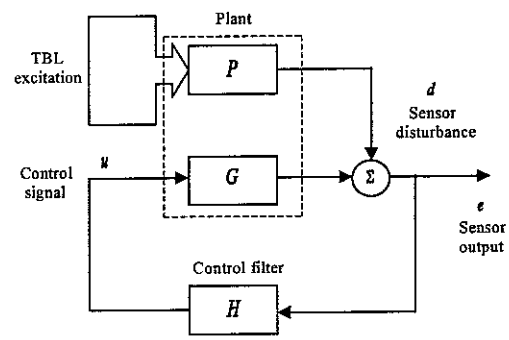

Figure 3: Principle of a feedback control system

The problem can be modelled by the scheme previously plotted in figure 3, where e is the sensor output error, d is the disturbance and u is the driving signal calculated to cancel the net volume velocity of the panel excited by a TBL. This driving signal will be sent through the plant G of the panel (representing the transfer function P between the sensor and the actuator) so that the error signal collected is $e = d + Gu$. Thus, the goal is to cancel the power spectral density of the total volume velocity S_{ee} measured at the sensor output.

This can be achieved assuming that the spectral characteristics of the secondary source strength must be given by:

$$S_{uu} = \frac{1}{|G(\omega)|^2} S_{dd}(\omega) \tag{25}$$

where S_{dd} is the power spectral density of the net volume velocity of the panel due to the primary excitation.

Here, the fact that the control filter H has to compensate for the behaviour G of the plant is stressed. Hence, a perfect rejection of the disturbance will be possible only if the plant is perfectly invertible, independently of the nature of the disturbance. This is the first limitation of the problem, because, in practice, the inversion of the plant response is altered by time delays in the controller. It can be shown that the plant response is perfectly invertible provided that collocated actuator/sensor pairs are used (ref [10]). In practice, if we want to cancel the volumetric contribution of the panel, this can be achieved by using a volume velocity sensor matched with a uniform force actuator. In principle, this configuration will generate a decrease in the sound power radiated without involving an increase in the near-field pressure levels (no control spillover).

If the feedback signal seems simple to obtain, the stability of the control filter has to be assessed in order to insure the feasibility of the control. The equivalent transfer function of such a feedback control is:

$$\frac{W(j\omega)}{F_p(j\omega)} = \frac{G(j\omega)}{1 + G(j\omega)H(j\omega)} \tag{26}$$

where $F_p(j\omega)$ is the primary excitation and $W(j\omega)$ is the measured net volume velocity of the structure. $G(j\omega)$ and $H(j\omega)$ are respectively the transfer functions of the mechanical system and of the feedback controller in the frequency domain. The point is that matched actuator/sensor paires have a minimum-phase transfer function, i.e. with both poles and zeros in the left hand side of the Laplace complex plane. Therefore, a controller transfer function that perfectly compensates for the plant response G, while including a large feedback gain α, will be given by $H(\omega) = -\alpha G^{-1}(\omega)$ and is also minimum-phase. Two major consequences are, first, that it doesn't accumulate phase when the frequency increases, i.e. no time delays, and second, that it remains stable whatever the magnitude of the feedback gain (unconditional stability) (ref [10,12,17]).

One more point of interest should be kept in mind. The main characteristic of an ASAC is that the control acts on the displacement not to reduce it but to reduce the noise induced by this one. Sometimes, a reduction of the noise can fit with an increasing of the vibration amplitudes.

As a conclusion for the active control strategy, it can be noticed that in order to suppress a random disturbance, a feedback control system is generally used. In practice, the efficiency of this strategy is improved by including another loop inside the first loop to come down to a feedforward control (internal model control). Such strategies will be presented in the part B of this report.

Part B: Simulation of the problem

Now that the basis of the problem are setted, it is possible to implement and investigate a control of the sound power radiated by the panel. Thus, the way used to program the problem will be presented in a first part. Then, an overview of the G. Gibbs results will be presented. Finally, the different strategies and their results will be exposed.

The reader should keep in mind that this study is only concerned with a single panel. Further studies may be led with a more accurate model (ref [24]).

B-1. Numerical formulation

The different expressions for the quantities of interest are known. The best way to compute them is now researched. Indeed, due to the complexity of the integrals required, the expressions have to be simplified before to be computed. The simulation will thus be semi-analytic. The main quantities required to calculate the spectrum of the kinetic energy of the plate and the acoustic power inwardly radiated are the matrices M and ψ of radiation efficiency and of modal excitation terms.

B-1-a- Expression of the radiation efficiency matrix

The M matrix represents the influence of an excitation on each structural mode. Its expression is a quadruple integral, that reveals:

$$M_{rsmn}(\omega) = \int_{x=0}^{b}\int_{y=0}^{a}\int_{x'=0}^{b}\int_{y'=0}^{a} \frac{4}{ab}\sin(\frac{r\pi x'}{b})\sin(\frac{s\pi y'}{a})\frac{\sin(k_0 R(M,M'))}{4\pi R(M,M')} \times \sin(\frac{m\pi x}{b})\sin(\frac{n\pi y}{a})dy'dx'dydx \tag{27}$$

The calculation of such an integral with a software like Matlab is quite long. Due to this fact, the expression has been simplified, using the method proposed by Mangiarotty in reference 25, before to be computed. The detail for the integral resolution is presented in annexe 1. Finally, the M matrix can be expressed after reduction as the following double integral:

$$M_{rsmn}(\omega) = \frac{4ab}{\pi}\int_{X_1=0}^{1}\int_{Y_1=0}^{1}\Phi(X_1,Y_1)F_{rm}(X_1)G_{sn}(Y_1)dX_1dY_1, \tag{28}$$

where:

$$\begin{cases} \Phi(X1,Y1) = \dfrac{\sin(k_0\sqrt{(bX_1)^2+(aY_1)^2})}{\sqrt{(bX_1)^2+(aY_1)^2}}, \\ F_{rm}(X_1) = \displaystyle\int_{X_2=0}^{1-X_1}\sin(r\pi X_2)\sin(m\pi(X_1+X_2))dX_2, \\ G_{sn}(X_1) = \displaystyle\int_{Y_2=0}^{1-Y_1}\sin(s\pi Y_2)\sin(n\pi(Y_1+Y_2))dY_2. \end{cases} \tag{29}$$

It is the calculation of the integral (28) that will be computed, using the following numerical approximation:

$$M_{rsmn}(\omega) = \frac{4ab}{\pi} \cdot \frac{1}{X_{\max} Y_{\max}} \sum_{k=1}^{X_{\max}} \sum_{p=1}^{Y_{\max}} \Phi\left(\frac{k}{X_{\max}}, \frac{p}{Y_{\max}}\right) F\left(\frac{k}{X_{\max}}\right) G\left(\frac{p}{Y_{\max}}\right) \tag{30}$$

where $X_{\max}$ and $Y_{\max}$ are the number of discretization points in the lateral and longitudinal directions. This number of point was optimized to be as small as possible to reduce the calculation time and as large as possible to provide a good approximation.

The results obtained with this method have been compared with these obtained by Maury (ref 4) and Wallace (ref 26). The representations of different coefficients are shown in annexe 3-a. The similarities between these coefficients permits to validate the model of the radiation efficiency terms matrix.

B-1-b- Expression of the modal excitation terms

In the same way, the expression of the excitation terms matrix ψ required to solve a quadruple integral, that reveals:

$$\psi_{rsmn}(\omega) = 4\pi^2 \int_{x=0}^{b} \int_{y=0}^{a} \int_{x'=0}^{b} \int_{y'=0}^{a} \frac{4}{ab} \sin\left(\frac{r\pi x'}{b}\right) \sin\left(\frac{m\pi x}{b}\right) \sin\left(\frac{s\pi y'}{a}\right) \sin\left(\frac{n\pi y}{a}\right) \times \phi_0(\omega) e^{-\alpha_x \left|\frac{\omega(x'-x)}{U_c}\right|} e^{-\alpha_y \left|\frac{\omega(y'-y)}{U_c}\right| - j\omega\frac{y'-y}{U_c}} dy'dx'dydx \tag{31}$$

It is possible to calculate it analytically, which will dramatically improve the computational cost of the program. In fact, this integral is a product of two double integrals: one depending on the variables x and x' and the other on the variables y and y'. The details of this calculation are explained in annexe 2.

B-1-c- Expression of the sound power radiated

It has been shown part A-3-b that the sound power inwardly radiated by the panel can be written as follow:

$$S_{\pi^-} = \frac{\omega \rho c}{2} Tr\left\{diag(A)^H \Re(M) diag(A) \Psi\right\} \tag{32}$$

The results issued from this expression have been compared with the experimental measurements of G. Gibbs (annexe 3-b). It should be noticed that for these measurements, the first peak should not be considered as it is due to the effect of the lateral panels superposed to the main one. Indeed, in this study, the choice of a single panel was made. A simplification can be applied to the expression (32), considering the matrices M and Ψ as diagonal matrices. These approximation, also called *diagonal approximation*, is equivalent to neglect the influences between the

structural modes. Figures of the sound power radiated with and without the diagonal approximation are plotted in annexe 3-c. It is shown that the amplitude of the peaks are not affected by the approximation, especially in the low frequency domain. Thus, this approximation will be used in all results shown in this study.

B-2. Results of the G.P.Gibbs Feedback Control Experiment

Due to the complexity of the experiment and to the fact that the control of TBL induced noise is a recent study, there are not a lot of results on this subject. As G. Gibbs *et al.* have achieved a complete experiment, the authors are interested in carrying feedback control simulation in order to compare both results. If those results are similar enough, it would be interesting to implement it on a real problem, with appropriate sensors and actuators and as a final aim, to design a real feedback equipment for the aeronautical industry.

It is important here to present briefly the results obtained by G. Gibbs at the NASA Langley Research Center. A summary of the results of two main studies (ref [27] and [28]) will be exposed. The first one was concerned by an active control in two panels and the second one aimed at reducing the number of sensors and actuators used.

To build their experiments, two single panels representing an aircraft structure have been mounted in a wind tunnel side. Below these panels, an anechoic enclosure has been installed. Then, the strategy was to pass the signals in a RME system that express the problem in the radiation modes basis (ref [29]), to keep only the influence of the radiation modes 1 to 7 (that are of main importance), and then to apply a feedback control on the two different panels separately or considered as one. The results of these two studies were the same. It stresses the fact that it is a good approximation to say that the different panels of an aircraft structure radiate separately. In each situation, an excitation has been applied for two different flight conditions, at Mach 0.8 and at Mach 2.5. In these first series of studies, 3 actuators and 15 sensors per panel have been used. The results showed reductions of about 10-20 dB at structural resonances and 5-10 dB integrated over a bandwidth of 150-800 Hz.

The main conclusions of this first study were that the RME method is performant, both panels can be controlled independently, and the feedback control system is really efficient, even with a random broadband noise as the one induced by a TBL.

A second study was then achieved in order to reduce the number of sensors and actuators. Actually, on commercial aircraft, there are hundreds of sidewall panels, so the number of sensors and actuators required can be a major problem (weight, electronics). The results were really convincing because it was shown that it is possible to reduce the control system required to 1 actuator and 4 sensors per panel. With such a strategy, the reductions in sound power were of about 10-15 dB at resonances, and of about 9 dB integrated over the control bandwidth of 150-800 Hertz (ref [27,28]).

B-3. Application of different active control strategies

As a random field, the excitation spectrum is defined by its power spectral density. Then, an expression of the sound power radiated can be extracted. In a first step, it is this quantity which will be of interest. We will thus simulate some feedback control in order to reduce it. First of all, actuators and sensors should be chosen to reduce vibrations. Then, an efficient control signal will be looked for.

B-3-a- Choice of the actuators and sensors

There are as many control strategies available as different kind of actuator and sensor pairs. In this study, we have chosen the same components as the ones used by G. Gibbs. In such a way, it is possible to compare the final results with measurements. These components are 15 accelerometers regularly distributed on the plate for the sensors, and 3 piezoelectric actuators. The geometry of the problem is shown on the figure 4:

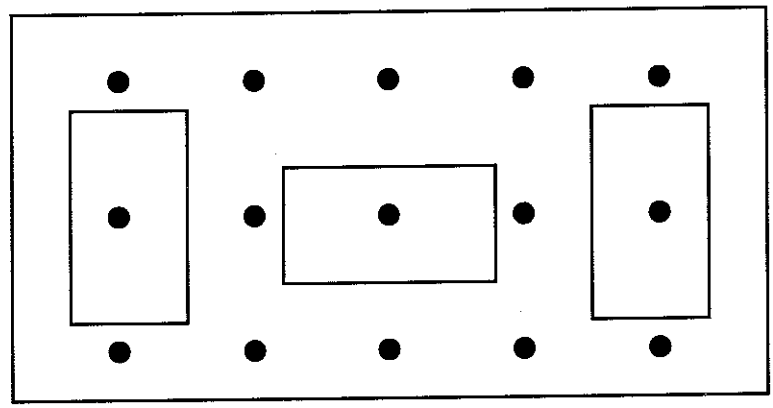

Figure 4: Distribution of the actuators/sensors in the panel

Due to the random aspect of the excitation, the quantity of interest for the control will not be the electric signal to apply to the actuators but its power spectral density. Let us denote this signal W.

H_{act} and H_s are respectively the transfer functions of the actuators and of the sensors. The expressions of such transfer functions are given (ref [12, 19]) by their modal terms:

$$H_{act_{mn}} = \left(\frac{S_{FF}}{S_{uu}}\right)_{mn} = \frac{C}{mn}(k_m^2 + k_n^2)(\cos[k_m x_1] - \cos[k_m x_2])(\cos[k_n y_1] - \cos[k_n y_2]) \quad (33)$$

$$H_{s_{mn}} = \left(\frac{S_{uu}}{S_{vv}}\right)_{mn} = -\omega^2 \sin(\frac{m\pi x_a}{l_x}) \sin(\frac{n\pi y_a}{l_y}) \quad (34)$$

where:

$$\begin{cases} C = \textit{constant depending on the material properties} \\ \quad \textit{of the plate and the piezoelectric material} \\ mn = \textit{order of the mode} \\ \\ x_1, y_1, x_2, y_2 = \textit{coordinates of the actuators} \\ x_a, y_a = \textit{coordinates of the sensors} \\ l_x = x \textit{ dimension of the plate} \\ l_y = y \textit{ dimension of the plate} \\ k_m = \dfrac{m\pi}{l_x} \\ k_n = \dfrac{n\pi}{l_y} \end{cases} \tag{35}$$

With such a model of our problem, an active control strategy can be applied to choose the parameter W.

Above all, in order to check if the model of the actuators is efficient, the influence of a single actuator excitation on the volume velocity of the plate was studied. These results were compared with the ones found by G. Gibbs. The figures of this calculation can be found in annexe 3-d. We can see that the actuators model used for this study is relevant. It should be considered that the first peak of the experimental results is due to the influence of the bigger panel. In fact, for the low frequencies, the transfer function between the actuator and the plate volume velocity is similar. Moreover, the phase of this transfer function is setted between $\pm\frac{\pi}{2}$ below 1000 Hertz (annexe 3-d3), which insures that the control will be stable for such frequencies, whithout implying big approximations in the secondary signal calculation.

B-3-b- Single feedback loop control

As a first step, the basic feedbak control strategy is studied.

The aim is to reduce the radiated sound power. As shown previously, the expression of this latter quantity before control can be expressed as follows:

$$S_{\pi^-} = \frac{\omega \rho c}{2} Tr\left\{diag(A)^H \Re(diag[M])diag(A)diag(\Psi)\right\} \tag{36}$$

The equivalent diagram related to this first strategy is shown in the figure 5.

With this loop, the expression of the sound power radiated becomes:

$$S_{\pi^-} = \frac{\omega \rho c}{2} Tr\left\{\Re(diag[M][I + AA' H_{act} W H_s]^{-1} AA'\Psi\right\} \tag{37}$$

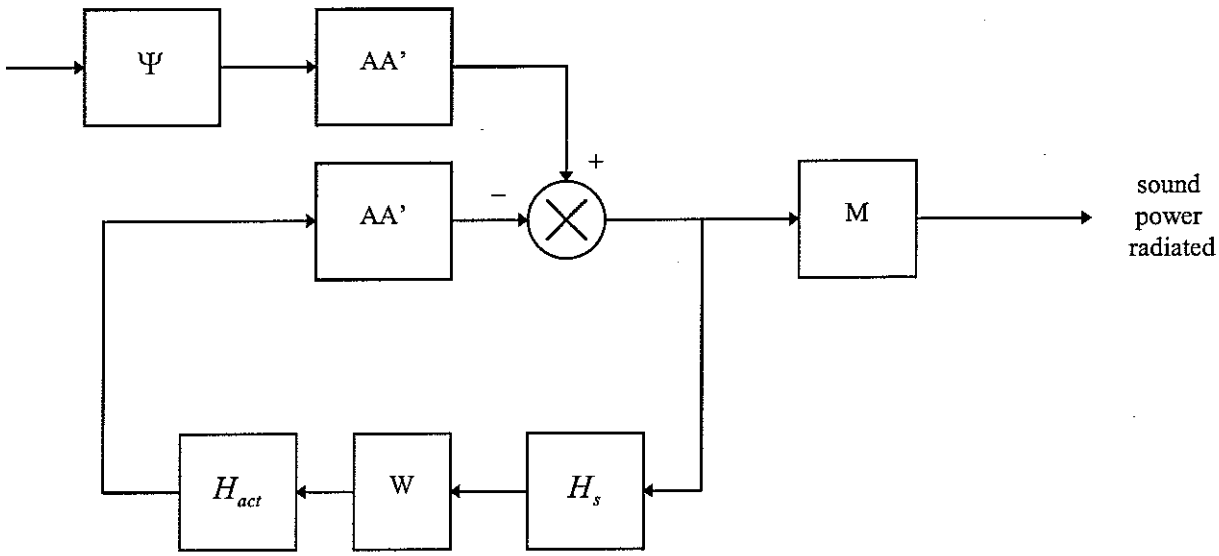

Figure 5: diagram of the problem

The main problem limiting the control is the fact that $[I + AA' H_{act} W H_s]$ has to be inverted. If A was invertible, it would be sufficient to take $W = -\frac{\alpha}{AA'}$, with $\alpha >> 1$, to ensure a large cancelation of the sound power radiated. Unfortunately, usually it is not the case. We will see that in order to avoid the inversion of A, the single feedback loop can be improved to transform the problem as a feedforward one.

B-3-c- The Internal Model Control: IMC

One of the main issue of the single feedback loop is that the plant response is modelled by the matrix A. An error in this matrix will be fed back into the loop and amplified. This can involve an large error. To avoid this problem, a second loop can be added to the first one (ref [30]). In such a way, the error induced by the approximation of the system response is cancelled. The control function acts directly on the quantity of interest, which improves the efficiency of the control. The representation of this Internal Model Control (IMC) loop is then shown in figure 6. In particular, it is assumed that a perfect plant model is available, which is not always the case in practical studies. For more informations about the IMC, the references 12, 17, 31 and 32 can be consulted.

The equivalent transfer function of this loop is given by:

$$\frac{s}{d} = (I - AA' H_{act} W H_s) \tag{38}$$

It is interesting to note that adding this second loop is equivalent to replace the inversion by a quadratic form (this is an approximation of the inversion).

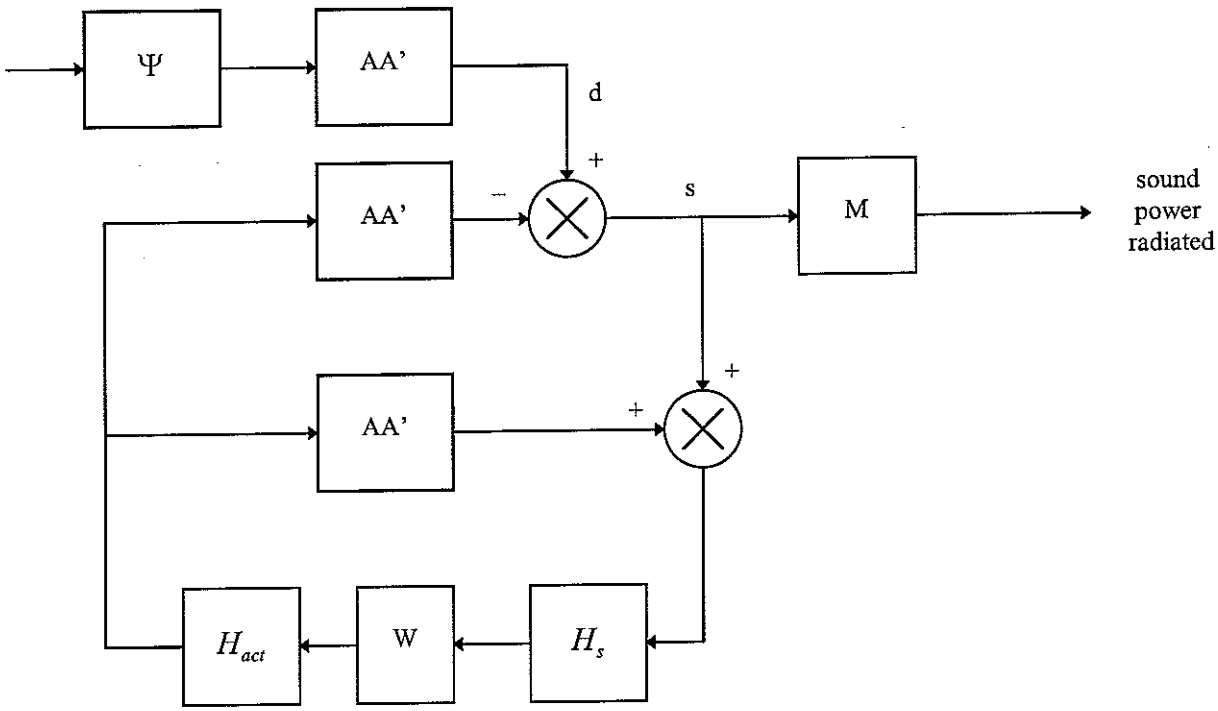

Figure 6: Internal Model Control

This expression permits to represents the feedback problem as a feedforward system in the following scheme 7.

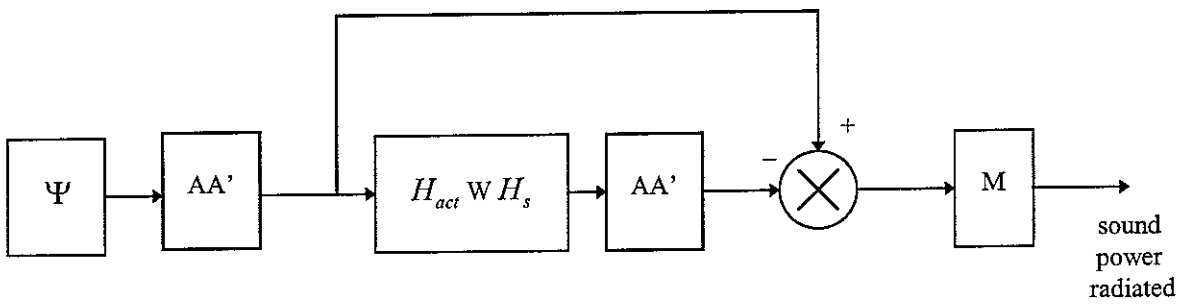

Figure 7: diagram of the problem

Thus, the sound power radiated can be expressed as:

$$S_{\pi^-} = \frac{\omega \rho c}{2} Tr\left\{\Re(diag[M])[I - AA' H_{act} W H_s] AA' \Psi\right\} \tag{39}$$

With this expression, it appears that choosing W to be equal to $1/\left[AA' H_{act} H_s\right]$ is the more efficient strategy because it will cancel completely the

disturbance. Unfortunately, in practice, this kind of control is not robust, so another value of W has to be found. For this reason the optimal value of W will be calculated minimizing the cost function J:

$$J = S_{\pi^-}^2 + \beta W^T W \tag{40}$$

The parameter β will be chosen as small as possible to optain a good cancelation of the noise, but large enough to insure the robustness of the control.

The expression of $\frac{\partial J}{\partial W}$ in respect with $W(\omega)$ is then calculated to find the optimal value of W that reduces J (annexe 4). The result is:

$$W_{opt} = \frac{1}{AA' H_{act} H_s + \frac{\beta}{H_{act}^{'} AA' M' MAA' \Psi\Psi' AA' H_s^{'}}} \tag{41}$$

The reduction obtained with such a strategy will be discussed in the next part.

At this point, the control strategy problem is well defined. It is then possible to simulate some controls and to analyse the results. The next part will present these results in detail together with comparisons with the G. Gibbs experiments.

Part C: Results

The previous work enables to have a relevant model for a control system acting on a panel excited by a TBL excitation. This part will present the results obtained from this model. In a second part, the efficiency and limitations of the problem will be presented.

C-1. Reduction obtained with the IMC

As a first step in the control calculations, the IMC was directly apply to the sound power radiated. This control reduces the contribution of all the modes. The result is shown in figure 8:

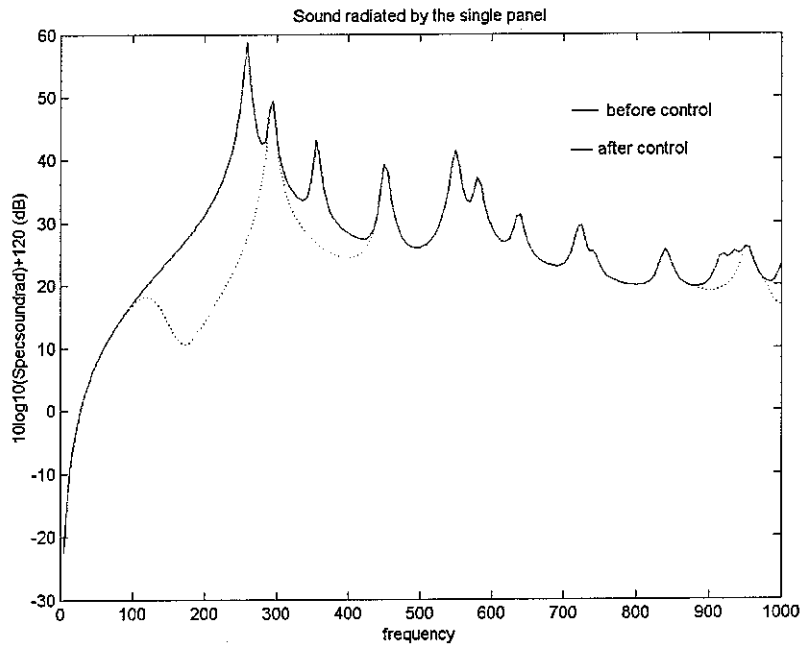

Figure 8: Feedback control of the sound power radiated

Here it appears that the first and third peaks corresponding to the first and third structural modes are reduced. The odd modes are not affected by the control due to the symmetrical position of our sensors and actuators. This theoretical result shows that the feedback strategy is efficient and can permit to obtain important reduction of the noise. In particular, this figure shows that with such a control the first peak in the sound power radiated spectrum can be cancelled. This is of real importance as this peak is the more important one. Moreover, the presence of peak in a spectrum is synonym of discomfort for the ears of the aircraft passenger in our case. Thus, the cancellation of one peak appears to be important.

C-2. Comparison between the theoretical control and the experimental one

The final comparison between the theoretical results and the experimental ones obtained by G. Gibbs can now be achieved. This comparison enables to validate or not the results obtained in this study. One of the experimental result of G. Gibbs considers the control of the first radiation mode. Hence, a control system acting only on this mode was implemented. In fact, an eigenvalue/eigenvector decomposition has been performed on the modal efficiency matrix, and only the components of the largest eigenvalue were kept. The theoretical result is shown in figure 9 and the G. Gibbs result is shown in figure 10.

The first peak appearing in figure 10 should not be considered, it is due to the experimental parameters. The main characteristic of the experimental result of G. Gibbs for this strategy (1 radiation mode) is that there is a spillover effect between 450 and 550 Hertz. With the theoretical result, it is possible to observe some spillover, but above 350 Hertz. This difference can be explain by the fact that during the experiment, the studied panel is embedded in a large panel. It is surrounded by other panels which imply some effect on it. This is just an hypothesis. It would be interesting to study a real panel in order to be able to compare the results. This will be the aim of further studies.

It can also be noted that in both figures, the attenuation of the first peak is about 15 - 20 dB. This result is the same in both studies and enhances the fact that a good reduction of the first peak in the sound power radiated spectrum can be obtained. This similarity appears in the low frequencies domain. Indeed, it is observed that the theoretical model is valid, at least for the low frequencies. The differences between the experiment and the theoratical parameters seem more and more important as the frequency increase.

Another point of interest in the comparison concernes the arrangement of the actuators. G. Gibbs showed that the number of actuators and sensors can be reduced without changing the results. A new configuration was thus adopted, where only the central actuator and four sensors distributed in diamond were kept, as shown in the figure 11.

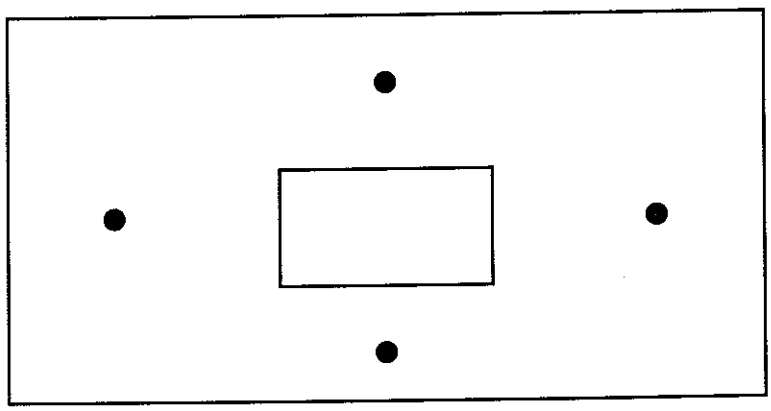

Figure 11: Simplest distribution of the actuators/sensors in the panel

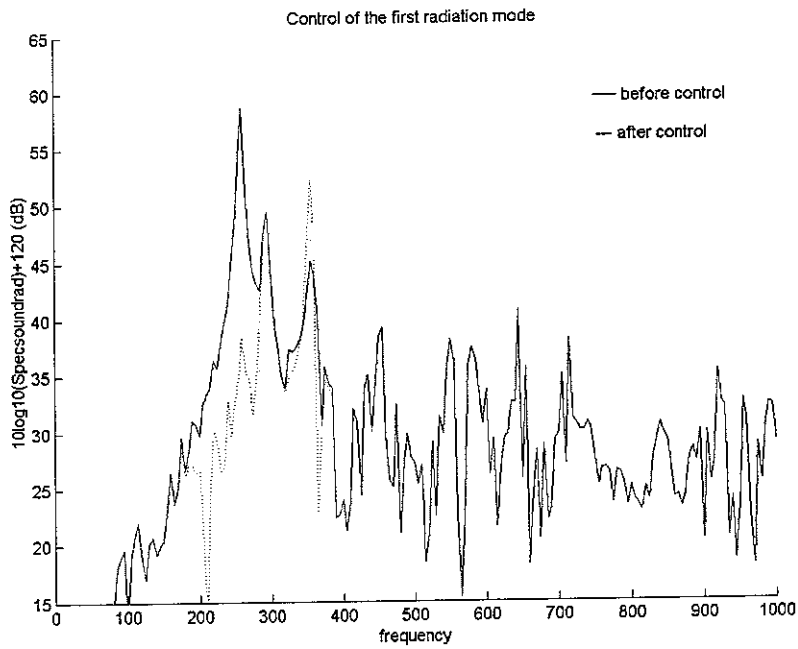

Figure 9: Control of the first radiation mode

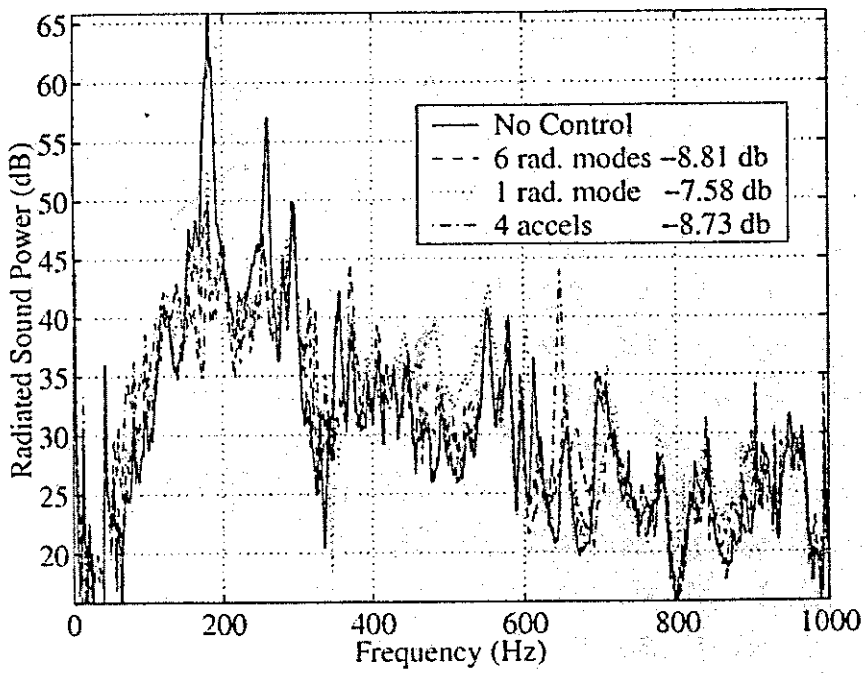

Figure 10: Control of the first radiation mode - G. Gibbs results

The application of the feedback control with the second actuator/sensor configuration provides almost the same result than with the first configuration, as it is shown in the figures 12 and 13.

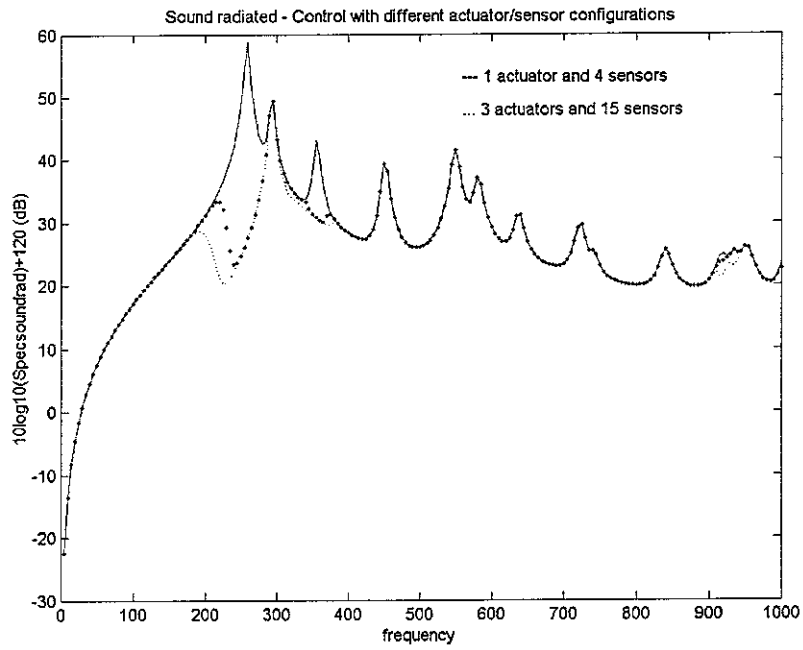

Figure 12: Comparison of the influence of two actuator/sensor configurations on the active control of the sound power radiated by the single panel

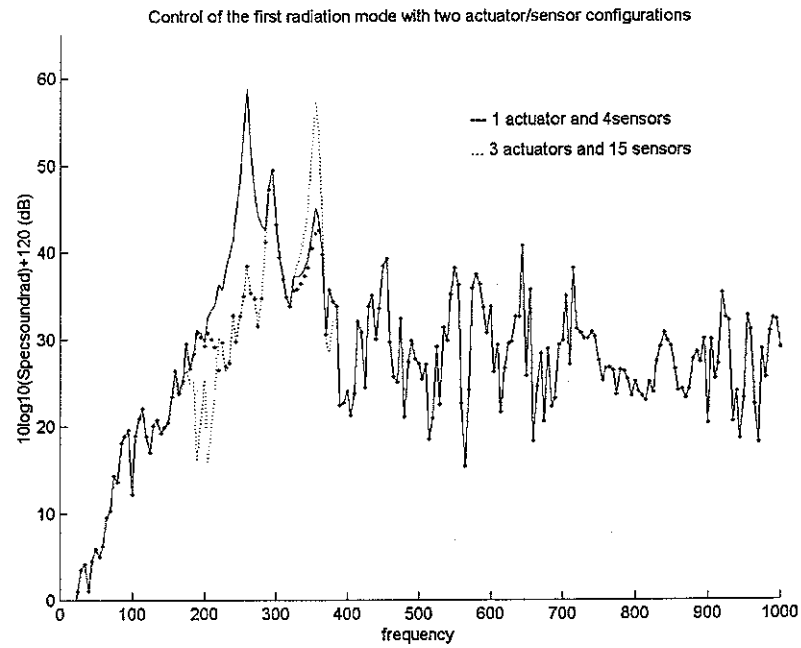

Figure 13: Comparison of the influence of two actuator/sensor configurations on the active control of the first radiation mode of the sound power radiated by the single panel

This implies that the number of actuators and sensors can be reduced. This result confirm the one obtained by G. Gibbs.

Finally, it has been shown that the experimental measurements of G. Gibbs and the theoretical results coincide well for the low frequencies. Above 1000 Hertz, it is more difficult to compare them. This can be explained by the numerous approximations used in the calculation which are valid up to a certain frequency. The fact that only a single panel is considered instead of a multi-panel fuselage can also imply some errors. Indeed, G. Gibbs studied a panel, but linked to other panels. Above a certain frequency, the approximation used in the theoretical model seems unjustified. Due to these reasons, some further studies will be achieved, assuming a double panel, or a single panel with reinforcements to make the model of the tensions inside the aircraft structure more accurate.

C-3. Influence of the suppression of different radiation modes

It has been shown that some reduction can be obtained by reducing the first radiation mode. Keeping the same actuators, it is interesting to see if results can be improved when more than one mode are considered.

The first radiation mode has the shape of a piston-like mode: this is why the configuration of our actuators can be efficient. It has to be noted that the contribution of the first radiation mode to the sound power radiated is proportional to the sum of the velocity of each point of the plate (the volumetric velocity).

The second and third radiation modes are rocking modes (ref 4), which means that they are symmetric with respect to the actuators positions. Due to this fact, they do not contribute to the volumetric velocity. In this way, acting on the first radiation mode will not change the contribution of the second and third radiation modes on the vibration of the plate. Nevertheless, the fourth mode, which is a quadrupole mode, contributes to the volumetric velocity. It will be excited in a different way when an anti vibration will be applied against the first mode. Due to this reason, it is possible that the control would be more efficient if we act on the fourth and first radiation modes together. A study was then led in this way. The results are plotted in figure 14.

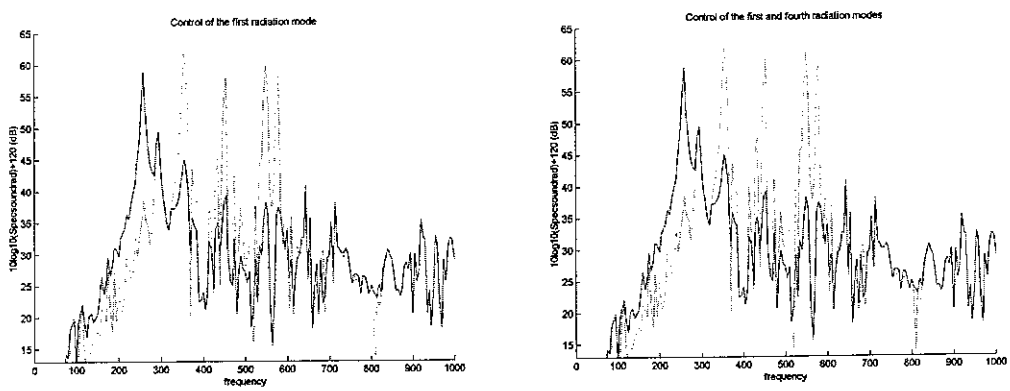

Figure 14: Influence of the firtst radiation mode alone and the first and fourth radiation modes

It appears that controlling the fourth radiation mode together with the first one is not useful. This can be explained by the fact that its influence on the sound power radiated is smaller than the one of the first mode. The strategy to consider only the first radiation mode is then justified.

C-4. The spillover effect

One of the physical mechanisms with active control is that it changes the energy distribution of the system. As a physical issue, there is an energy conservation. It means that a noise attenuation for certain frequencies can be associated with an increase in an other frequency domain. This is also called the spillover effect. Usually, this effect appears when one mode is controlled. The energy reduced on this mode will be set off again on the other modes, which imply a spillover. In this study, a spillover appears when we try to reduce the first radiation mode, but not when the strategy is to cancel the complete sound power radiated (figure 15).

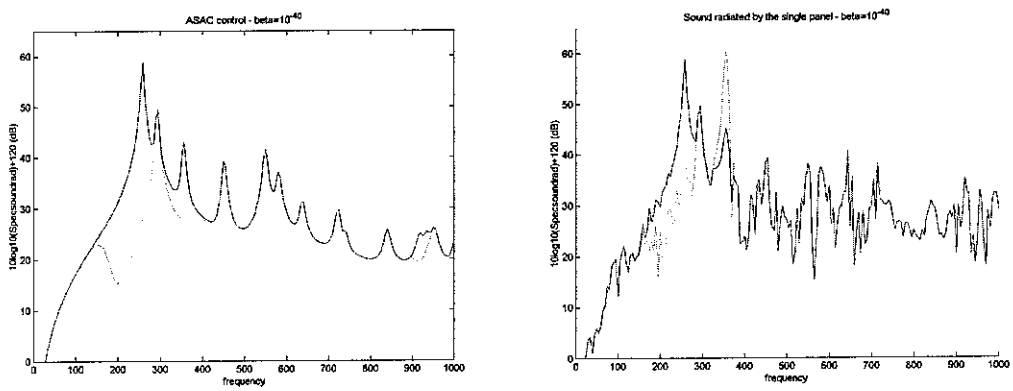

Figure 15: The spillover effect

An explanation for this phenomenon is that when we reduce only the first radiation mode, the energy can be redistributed again on the other mode and then imply some spillover. When the complete sound power radiated is controlled, it looks like if each radiation mode was controlled, then the energy is not transmitted directly to other modes. Nevertheless, the energy conservation should be ensured. Some spillover will not appear, but the performance of the control will be worse. The energy repartition will be on all the modes, decreasing the efficiency of the control on each mode.

C-5. Robustness of the control

Another point of interest in the active control strategy is the robustness of the control. In fact, as a consequence of the approximations used to calculate the control signal, there is a risk to implement an unrobust control. This corresponds to a control where the error on the calculation grows up at each time step to end up at a large secondary signal, too important for the control.

For this reason, a criterion to control the robustness was researched. It has been shown that in order to obtain a robust control the complementary sensitivity function T should respect the inequation (42).

$$T < \frac{1}{B} \tag{42}$$

where B is a constant representing the precision chosen for the stability criterion. A usual value of B is 0.5.

Some complementary functions were plotted, for different value of the β coefficient in equation (40). It appears (figure 16) that as expected, the smaller the β, the better is the control, but the worse is its robustness. A compromise is then found. This is the object of the next part C-6.

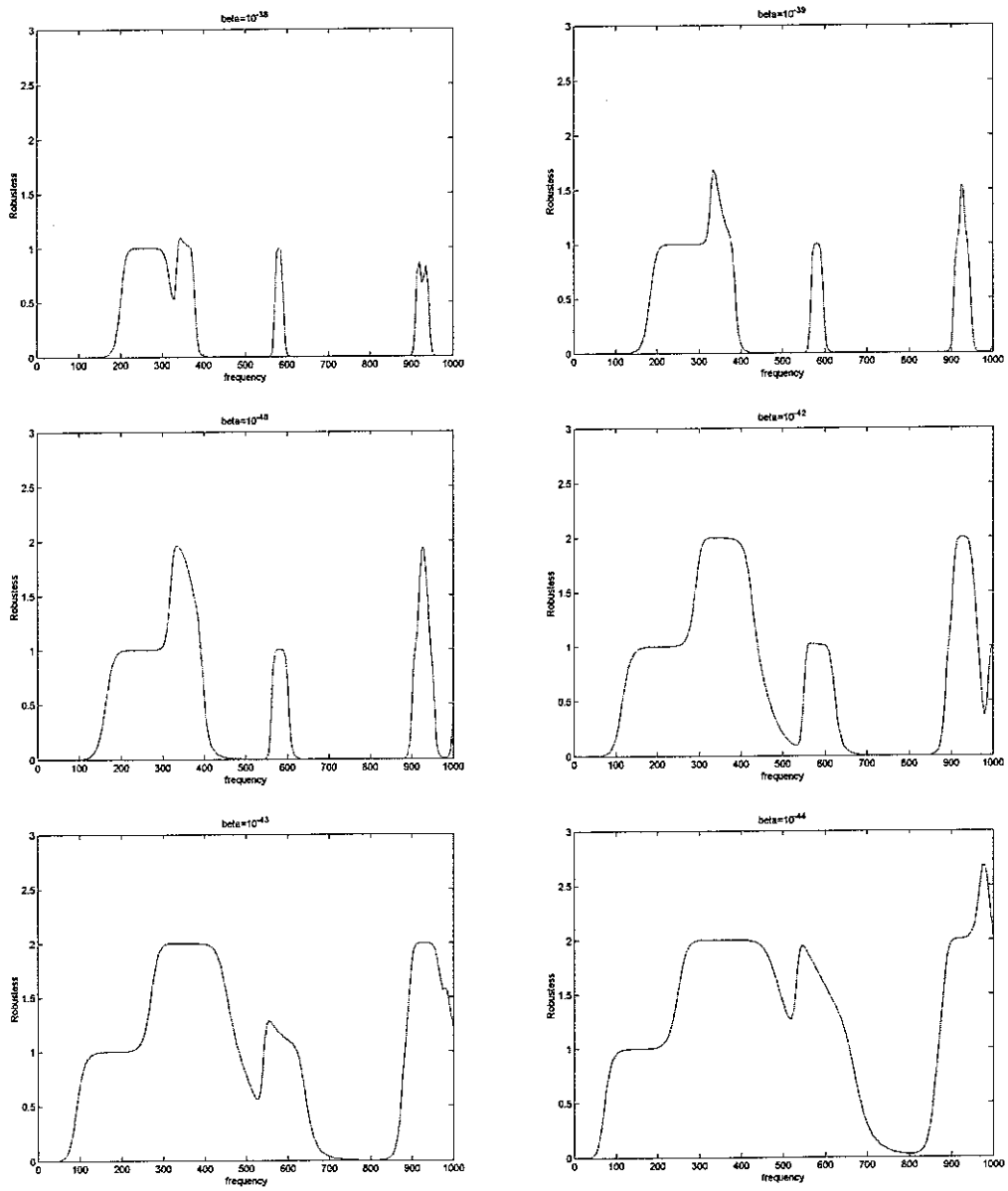

Figure 16: Influence of β on the control robustness

The complementary sensitivity function is defined in equation (43).

$$T = \left| AA' H_{act} W H_s \right| \tag{43}$$

More information about the complementary sensitivity function and the robustness of a control can be found in reference [30].

C-6. Influence of the β parameter

It has been shown that one of the main parameter of our feedback control is the β coefficient appearing in equation (40). This coefficient reduces the efficiency of the control as it changes the cost function. On the other hand, it makes the control feasible, controlling its input and permitting it to be stable.

It should be consider that the control is applied by several actuators. A theoretical calculation of the signal to apply does not take care about the limitations of such materials. If the cost function (equation (40)) was not attenuated by the second term, dependant on the β coefficient, the cost of the control would be some very large electrical signals sent at the input of the actuators. This would be impossible to apply, even if the results would be really efficient. Due to this reason, the β coefficient should be chosen big enough to ensure a feasibility of the control. Moreover, the fact to apply a big coefficient will permit to ensure the stability and robustness of the control as shown in the previous part C-5.

Of course, the final aim is to control the square of the sound power radiated $S_{\pi^-}^2$. So if a good cancellation is researched, the cost function (equation (40)) should be as close as possible from it. It is then clear that the control will be better with a smaller β coefficient.

Such remarks were already denoted by Thomas and Nelson (reference [33]) where it appears that when β decreases, the control becomes better and the spillover increases. The same conclusions are pointed out in our study as shown in the following figure 17.

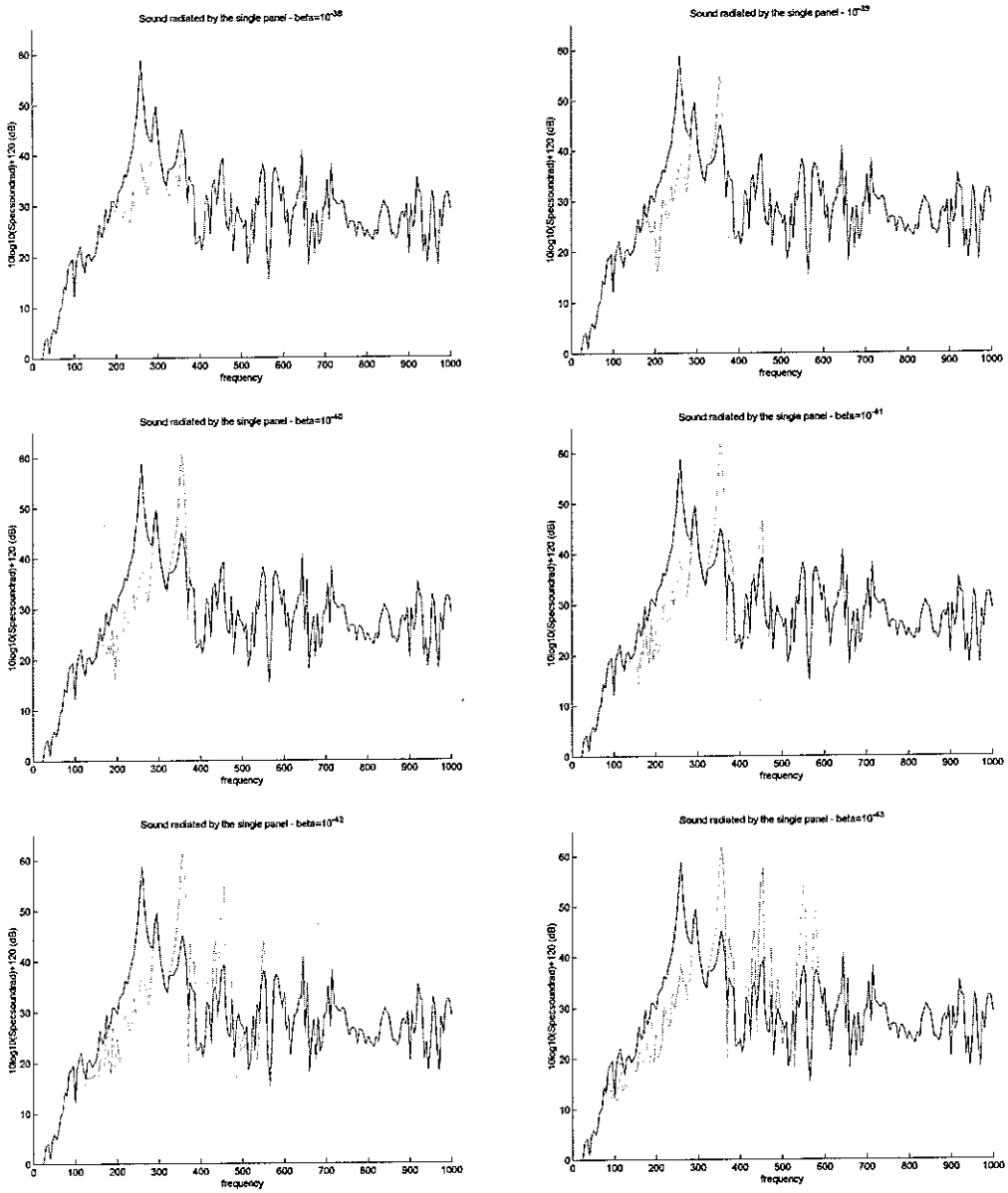

Figure 17: Influence of the β coefficient on the control of the sound power radiated

Figure 18 also stresses this result showing that bigger is the β coefficient, better is the efficiency of the control.

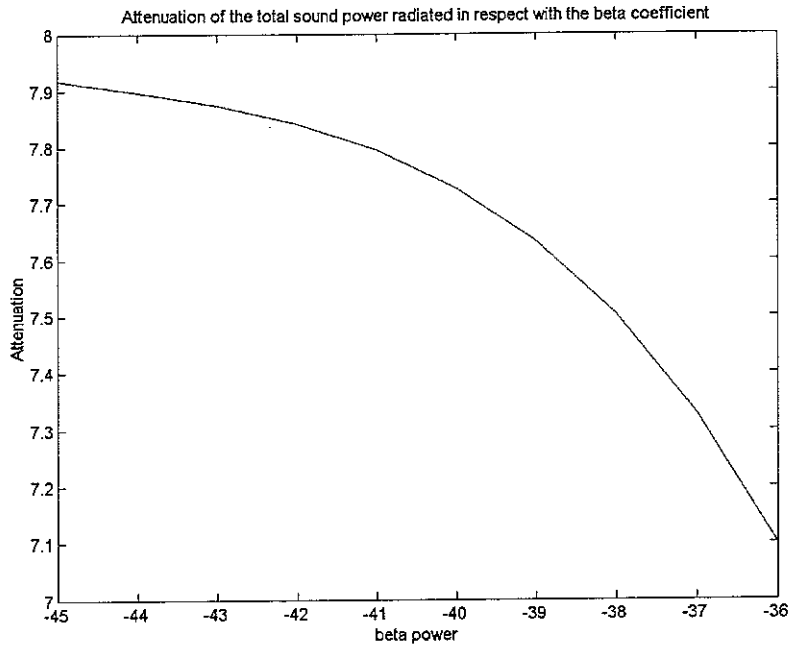

Figure 18: Attenuation of the total sound power radiated in respect with the β coefficient

C-7. Validity of several approximations

Due to the fact that a semi-analytic approach has been chosen, several approximations were assumed in the calculation of the sound power radiated. Fortunately their influence on the result can be neglected.

C-7-a- Diagonalisation of the matrices M and Ψ

As a first approximation on the radiation efficiency matrix M and on the modal excitation terms matrix Ψ, all the matrices are assumed to be diagonal. This approximation is equivalent to consider that the cross terms are neglected with respect with the diagonal terms. As the influence between the different modes is not that important, this approximation is justified. This is illustrated by the following figure 19.

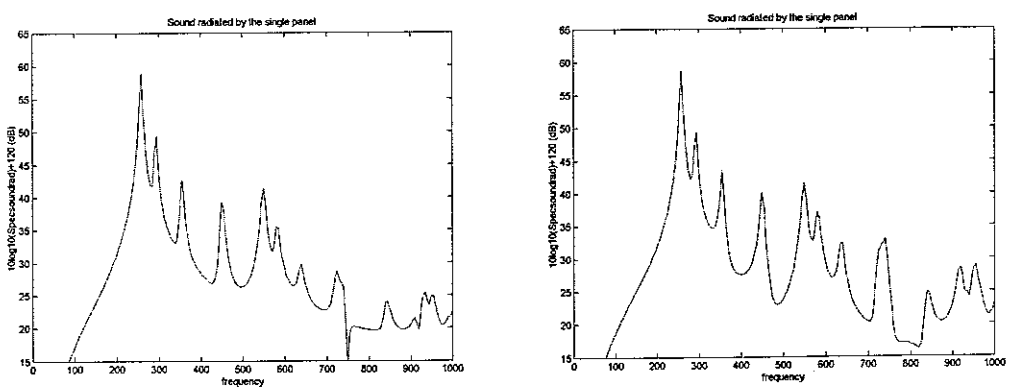

Figure 19: Justification of the diagonalisations

C-7-b- Factorisation of the matrix M

When the first radiation mode is concerned, a factorisation of the radiation efficiency matrix M has to be applied. This factorisation is described in equation (23). As the M matrix is not completely symmetric and positive (due to approximations), the factorisation implies some error, but this error is less important for the low frequencies domain. To be sure that this approximation is well justified, the sound power radiated was calculated with and without approximation in figures 20.

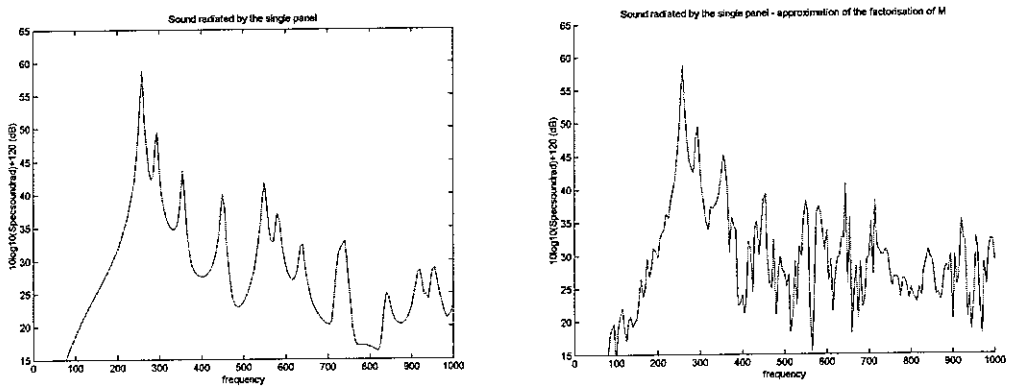

Figure 20: Justification of the approximation of the M factorisation

C-8. Calculation time

One of the main characteristic of the approach used in this study is that it is semi-analytic. It is not possible to calculate exactly all the integrals required by such a problem. In the other hand, the calculation time would be really important if a completely analytic approach was chosen. Due to these reasons, the problem was computed in a semi-analytic way (cf B-1).

In one hand, this approach is better as it avoids some approximations. In the other hand, it permits a fast calculation. This is enlightened by the calculation time values given in figure 21. These values represent the time required by the calculation of the sound power radiated with and without control in different conditions.

frequency range: **frequency step:**	**0 --> 1000 Hz** **5 Hz**	**0 --> 1000 Hz** **1 Hz**	**0 --> 5000 Hz** **5 Hz**	**0 --> 5000 Hz** **1 Hz**
time calculation	1 min.32 sec.	7 min.35 sec.	7 min.35 sec.	38min.

Figure 21: Calculation time of the problem

As the frequency range of interest is below 1 kHertz and as a frequency step of 5 Hertz is enough to obtain exact results, these calculation times are a good proof of the efficiency of the method used in this study.

Conclusions

At present time, computer facilities allow to model the response of a panel excited by a turbulent boundary layer. Without mounting an experiment in a wind tunnel, it is possible to simulate the flow-induced noise transmitted through a panel. This is really interesting for the study of sound power radiated in aircraft structure due to the exterior turbulent boundary layer because a plane fuselage can be viewed as a set of panel radiating independently. As a first step, this study is concerned with a simple structure, but in the future, aircraft skins will be modelled as a double layer panel. This is currently under study at the Institute of Sound and Vibration Research of Southampton (ref [24]).

Then, as a model of the problem is available, some control strategies with different actuators and sensors were simulated. The control can either suppress the first structural modes, or the first radiation modes. Experiments were achieved and compared with the ones of G. Gibbs. The comparison is difficult due to the differences between a theoretical and an experimental study. However, both results agree. It is shown that a feedback control, using an internal model control loop, allows to obtain efficient cancellation of the noise inwardly radiated by a panel excited by a TBL, and this with few actuators and sensors. This study shows the validity of the theoretical model and the possibility for the plane manufacturers to envisage an efficient robust control of the aerodynamic noise.

At least, this is a simple model of aircraft structure due to approximations. New research axis can be the study of a more complete aircraft model with for example a double layer panel, or the study of sensors and actuators design to test feedback control. This is of great interest for aeronautical manufacturers because of the need to improve the passengers' comfort and to satisfy stringent norm levels.

References:

1. W.R. Graham, "A Comparison of Models for the Wavenumber-Frequency Spectrum of Turbulent Boundary Layer Pressures", *Journal of Sound and Vibration*, **206** (4), 1997, p.541-565.
2. W.R. Graham, "Boundary Layer Induced Noise in Aircraft, Part I: the Flat Plate Model", *Journal of Sound and Vibration*, **192** (1), 1996, p.101-120.
3. W.V. Bhat, and J.F. Wilby, "Interior Noise Radiated by an Airplane Fuselage Subjected to Turbulent Boundary Layer Excitation and Evaluation of Noise Reduction Treatments", *Journal of Sound and Vibration*, **18** (4), 1971, p.449-464.
4. C. Maury, P. Gardonio and S.J. Elliott, "Model for the Control of the Sound Radiated by an Aircraft Panel Excited by a Turbulent Boundary Layer", *ISVR Technical Report* No **287**, June 2000.
5. G.M. Corcos, "The Structure of the Turbulent Pressure Field in Boundary Layer Flows", *Journal of Fluid Mechanics*, **18**, 1964, p.353-378.
6. G.M. Corcos, "Resolution of Pressure in Turbulence", *Journal of the Acoustical Society of America*, **35** (2), February 1963, p.192-199.
7. B.M. Efimtsov, "Characteristics of the Field of Turbulent Wall Pressure Fluctuations at Large Reynolds Number", *Soviet Physics Acoustics*, **28** (4), 1982, p.289-292.
8. A. Preumont, "Random Vibration and Spectral Analysis", Kluwer Academic Publishers, Solid Mechanics and Its Applications, Vol.33, chap 6.8.
9. W.V. Bhat, "Flight Test Measurement of Exterior Turbulent Boundary Layer Pressure Fluctuations on Boeing Model 737 Airplane", *Journal of Sound and Vibration*, **14** (4), 1971, p.439-457.
10. C. Maury, P. Gardonio and S.J. Elliott, "Active Control of the Flow-Induced Noise Transmitted Through a Panel", *Proc.of the 6th AIAA/CEAS Aeroacoustics Conference*, AIAA 2000-2042.
11. W.R. Graham, "The Influence of Curvature on the Sound Radiated by Vibrating Panels", *Journal of the Acoustical Society of America*, **98**(3), 1995, p.1581-1595.
12. C.A. Fuller, S.J. Elliott and P.A. Nelson, "Active Control of the Vibrations", London: academic, 1996.
13. M.E. Johnson, J. Griffin and C.R. Fuller, "Experiments on Feedforward Control of Turbulent Boundary Layer Noise", *Proceedings of Active 99*, Ft.Lauderdale, FL, Dec 2-4, 1999, p.435-445.
14. S.J. Elliott and M.E. Johnson, "Radiation Modes and the Active Control of Sound Power", *Journal of the Acoustical Society of America*, **94** (4), October 1993, p.2194-2204.
15. G.P. Gibbs, R.L. Clark, D.E. Cox, and J.S. Vipperman, "Radiation Modal Expansion: Application to Active Structural Acoustic Control", *Journal of the Acoustical Society of America*, **107** (1), 2000, p.332-339.
16. E. Friot, and M. Georgelin, "Contrôle actif des vibrations d'une plaque excitée par un écoulement turbulent", rapport interne Laboratoire de Mécanique et d'acoustique de Marseille.
17. P.A. Nelson, and S.J. Elliott, "Active Control of Sound", London: academic, 1992.

18. G. Guigou and C.R. Fuller, "Control of Aircraft Interior Broadband Noise with Foam-PVDF Smart Skin", *Journal of Sound and Vibration*, **220** (3), 1999, p.541-557.
19. T.C. Sors and S.J. Elliott, "Modelling and Feedback Control of Sound Radiation from a Vibrating Panel", *Smart Mater. Struct.*, **8**, 1999, p.301-314.
20. E.K. Dimitriadis, C.R. Fuller, and C.A. Roger, *Transaction of the* ASME, *J. Vib. Acoust.* **113**, p.100-107.
21. S.D. Snyder, C.H. Hansen, and N. Tanaka, Proc. "2nd Conf. on Recent Advances in Active Control of Sound and Radiation", 1993, p.177-188.
22. M.E. Johnson, and S.J. Elliott, 1995, *Proc.* SPIE **2443**, p.658-669.
23. M.E. Johnson, and S.J. Elliott, "Active Control of Sound Radiation Using Volume Velocity Cancellation", *Journal of the Acoustical Society of America*, **98** (4), 1995, p.2174-2186.
24. C. Maury, P. Gardonio, and S.J. Elliott, "Analysis of the Boundary Layer Noise Transmitted Through Aircraft Sidewalls", *Proc.of the 7th AIAA/CEAS Aeroacoustics Conference*, AIAA 2001.
25. R.A. Mangiarotty, "Acoustic Radiation Damping of Vibrating Structures", *Journal of the Acoustical Society of America*, **35**(3), March 1963, p. 369-377.
26. C.E. Wallace, "Radiation Resistance of a Rectangular Panel", *Journal of the Acoustical Society of America*, **51**(3), 1972, p. 946-952.
27. G.P. Gibbs, K.W. Eure and J.W. Lloyd, "Active Control of Turbulent Boundary Layer Induced Sound Radiation from Aircraft Style Panels", *Proceedings of Active 99*, **837**.
28. G.P. Gibbs, R.H. Cabell, and J. Juang, "Controller Complexity for Active Control of TBL Induced Sound Radiation from Panels", *American Institute of Aeronautics and Astronautics*, 12-14 June 2000, AIAA 2000-2043.
29. J.N. Juang and K.W. Eure, "Predictive Feedback and Feedforward Control for Systems with Unknown Disturbances", *NASA Technical Memorandum* **208744**, 1998.
30. S.J. Elliott, "Signal Processing for Active Control", Academic Press, 2001.
31. D.W. Clarke, C. Mohtadi, and P.S. Tuffs, "Generalized Predictive Control - Part I. The Basic algorithm", *Automatica*, **23** (2), 1987, p. 137-148.
32 S.J. Elliott, T.J. Sutton, B. Rafaely and M. Johnson, "Design of Feedback Controllers Using a Feedforward Approach", *Proceedings of Active 95*, 1995, p.863-874.
33. D.R. Thomas and P.A. Nelson, "On the Use of Feedback to Control Sound Radiation from a Plate Excited by a Turbulent Boundary Layer", *ISVR Technical Report* **227**, January 1994.

Annexes

Annexe 1: Calculation of the radiation efficiency matrix

The expression to be calculated for each element of the matrix M is the following one:

$$M_{rsmn}(\omega) = \int_{x=0}^{b}\int_{y=0}^{a}\int_{x'=0}^{b}\int_{y'=0}^{a} \frac{4}{ab}\sin(\frac{r\pi x'}{b})\sin(\frac{s\pi y'}{a})\frac{\sin(k_0 R(M,M'))}{4\pi R(M,M')} \times \sin(\frac{m\pi x}{b})\sin(\frac{n\pi y}{a})dy'dx'dydx. \quad \text{(A1-1)}$$

The calculation of such an integral can be simplified using the Mangiarotty method (ref 29).
The first step is to apply the next changing of variables:

$$\begin{cases} X = x - x' \quad , \quad x' = x', \\ Y = y - y' \quad , \quad y' = y'. \end{cases} \quad \text{(A1-2)}$$

The expression of M becomes:

$$M_{rsmn}(\omega) = \frac{4}{\pi ab}\int_{X=0}^{b}\int_{Y=0}^{a}\frac{\sin(k_0 R)}{R}\int_{x'=0}^{b-X}\int_{y'=0}^{a-Y}\sin(\frac{r\pi x'}{b})\sin(\frac{m\pi(X+x')}{b}) \times \sin(\frac{s\pi y'}{a})\sin(\frac{n\pi(Y+y')}{a})dy'dx'dYdX. \quad \text{(A1-3)}$$

where $R = \sqrt{X^2 + Y^2}$.

Then, a new changing of variables is applied:

$$\begin{cases} X_1 = X/b \quad , \quad X_2 = x'/b, \\ Y_1 = Y/a \quad , \quad Y_2 = y'/a. \end{cases} \quad \text{(A1-4)}$$

This leads to the following expression:

$$M_{rsmn}(\omega) = \frac{4ab}{\pi}\int_{X_1=0}^{1}\int_{Y_1=0}^{1}\Phi(X_1,Y_1)F_{rm}(X_1)G_{sn}(Y_1)dX_1dY_1 \, , \quad \text{(A1-5)}$$

where:

$$\begin{cases} \Phi(X1,Y1) = \dfrac{\sin(k_0\sqrt{(bX_1)^2+(aY_1)^2})}{\sqrt{(bX_1)^2+(aY_1)^2}}, \\ F_{rm}(X_1) = \displaystyle\int_{X_2=0}^{1-X_1} \sin(r\pi X_2)\sin(m\pi(X_1+X_2))dX_2, \\ G_{sn}(X_1) = \displaystyle\int_{Y_2=0}^{1-Y_1} \sin(s\pi Y_2)\sin(n\pi(Y_1+Y_2))dY_2. \end{cases} \quad \text{(A1-6)}$$

The expression for Φ will be directly computed, but the F and G integrals can be calculated analytically, following the same method. Here, the calculation of the F integral is only presented, but it is exactly the same with the G integral.

The integral to be calculated is:

$$F_{rm}(X_1) = \int_{X_2=0}^{1-X_1} \sin(r\pi X_2)\sin(m\pi(X_1+X_2))dX_2. \quad \text{(A1-7)}$$

It can be expressed as:

$$F_{rm}(X_1) = \frac{1}{2}\int_{X_2=0}^{1-X_1} \cos((m-r)\pi X_2 + m\pi X_1) - \cos((m+r)\pi X_2 + m\pi X_1)dX_2, \quad \text{(A1-8)}$$

and then

$$\begin{aligned} F_{rm}(X_1) = \int_{X_2=0}^{1-X_1} [&\cos((m-r)\pi X_2)\cos(m\pi X_1) \\ &- \sin((m-r)\pi X_2)\sin(m\pi X_1) - \cos((m+r)\pi X_2)\cos(m\pi X_1) \\ &+ \sin((m+r)\pi X_2)\sin(m\pi X_1)]dX_2. \end{aligned} \quad \text{(A1-9)}$$

Here, two different cases can be distinguished:

*If $m = r$:

$$F_{rr}(X_1) = (1-X_1)\frac{\cos(r\pi X_1)}{2} - \frac{\sin(r\pi(2-X_1)) - \sin(r\pi X_1)}{4\pi r}. \quad \text{(A1-10)}$$

*If $m \neq r$:

$$\begin{aligned} F_{rm}(X_1) = \frac{1}{2\pi(m^2-r^2)}\{&(m+r)[\sin((m-r)\pi + r\pi X_1) - \sin(m\pi X_1)] \\ &-(m-r)[\sin((m+r)\pi - r\pi X_1) - \sin(m\pi X_1)]\}. \end{aligned} \quad \text{(A1-11)}$$

Annexe 2: Calculation of the modal excitation terms matrix

This appendix shows the details of the theoretical calculation of the ψ matrix of the modal excitation terms. This calculation permits to compute the exact value of the integral. There are no approximations and it enables parametric studies to be performed at a low cost.

The integral we have to calculate is the following one:

$$\psi_{rsmn}(\omega) = 4\pi^2 \int_{x=0}^{b}\int_{y=0}^{a}\int_{x'=0}^{b}\int_{y'=0}^{a} \frac{4}{ab}\sin(\frac{r\pi x'}{b})\sin(\frac{m\pi x}{b})\sin(\frac{s\pi y'}{a})\sin(\frac{n\pi y}{a}) \times \phi_0(\omega) e^{-\alpha_x\left|\frac{\omega(x'-x)}{U_c}\right|} e^{-\alpha_y\left|\frac{\omega(y'-y)}{U_c}\right| - j\omega\frac{y'-y}{U_c}} dy'dx'dydx. \quad \text{(A2-1)}$$

This main integral is divided in two parts. ψ is the result of the product between the two expressions A and B, multiplied by $16\pi^2\phi_0 / ab$, where:

$$A = \int_{x=0}^{b}\int_{x'=0}^{b} \sin(\frac{r\pi x'}{b})\sin(\frac{m\pi x}{b}) e^{-\alpha_x\left|\frac{\omega(x'-x)}{U_c}\right|} dxdx', \quad \text{(A2-2)}$$

$$B = \int_{y=0}^{a}\int_{y'=0}^{a} \sin(\frac{s\pi y'}{a})\sin(\frac{n\pi y}{a}) e^{-\alpha_y\left|\frac{\omega(y'-y)}{U_c}\right| - j\omega\frac{y'-y}{U_c}} dydy'. \quad \text{(A2-3)}$$

As a first step, we apply the following variable transformation:

$$\begin{cases} X = x/b \quad , \quad X' = x'/b, \\ Y = y/a \quad , \quad Y' = y'/a, \end{cases} \quad \text{(A2-4)}$$

and so, expressions (A2-2) and (A2-3) become:

$$A = b^2 \int_{X=0}^{1}\int_{X'=0}^{1} \sin(r\pi X')\sin(m\pi X) e^{-\alpha_x\left|\frac{\omega b(X'-X)}{U_c}\right|} dXdX', \quad \text{(A2-5)}$$

$$B = a^2 \int_{Y=0}^{1}\int_{Y'=0}^{1} \sin(s\pi Y')\sin(n\pi Y) e^{-\alpha_y\left|\frac{\omega a(Y'-Y)}{U_c}\right| - j\omega a\frac{Y'-Y}{U_c}} dYdY'. \quad \text{(A2-6)}$$

Then, a second variable transformation is applied:

$$\begin{cases} X_1 = X'-X \quad , \quad X_2 = \frac{1}{2}(X+X'-1), \\ Y_1 = Y'-Y \quad , \quad Y_2 = \frac{1}{2}(Y+Y'-1). \end{cases} \quad \text{(A2-7)}$$

The new expression of A can be written as:

$$A = b^2 \int_{X_1=-1}^{1} \int_{X_2=\frac{|X_1|}{2}-\frac{1}{2}}^{\frac{1}{2}-\frac{|X_1|}{2}} \sin(r\pi(\frac{X_1}{2}+X_2+\frac{1}{2}))\sin(m\pi(-\frac{X_1}{2}+X_2+\frac{1}{2}))e^{-\alpha_x\left|\frac{\omega b X_1}{U_c}\right|}dX_1dX_2. \quad \text{(A2-8)}$$

Using trigonometric formula, this expression becomes:

$$\begin{aligned} A = \frac{b^2}{2} \int_{X_1=-1}^{1} \int_{X_2=\frac{|X_1|}{2}-\frac{1}{2}}^{\frac{1}{2}-\frac{|X_1|}{2}} & [\cos((r-m)\pi(X_2+\frac{1}{2}))\cos((r+m)\pi\frac{X_1}{2}) \\ & -\sin((r-m)\pi(X_2+\frac{1}{2}))\sin((r+m)\pi\frac{X_1}{2}) - \cos((r+m)\pi(X_2+\frac{1}{2}))\cos((r-m)\pi\frac{X_1}{2}) \\ & +\sin((r+m)\pi(X_2+\frac{1}{2}))\sin((r-m)\pi\frac{X_1}{2})]e^{-\alpha_x\left|\frac{\omega b X_1}{U_c}\right|}dX_1dX_2. \end{aligned} \quad \text{(A2-9)}$$

Then, two cases can be studied:

*case 1: If $r = m$:

$$A = \frac{b^2}{2} \int_{X_1=-1}^{1} \int_{X_2=\frac{|X_1|}{2}-\frac{1}{2}}^{\frac{1}{2}-\frac{|X_1|}{2}} [\cos(r\pi X_1) - \cos(2r\pi(X_2+\frac{1}{2}))]e^{-\alpha_x\left|\frac{\omega b X_1}{U_c}\right|}dX_1dX_2. \quad \text{(A2-10)}$$

The integration of this expression with respect to X_2 gives:

$$A = \frac{b^2}{2} \int_{X_1=-1}^{1} e^{-\alpha_x\left|\frac{\omega b X_1}{U_c}\right|}[(1-|X_1|)\cos(r\pi X_1) + \frac{1}{r\pi}\sin(r\pi|X_1|)]dX_1, \quad \text{(A2-11)}$$

or

$$A = b^2 \int_{X_1=0}^{1} e^{-\alpha_x\frac{\omega b X_1}{U_c}}[(1-X_1)\cos(r\pi X_1) + \frac{1}{r\pi}\sin(r\pi X_1)]dX_1. \quad \text{(A2-12)}$$

Writing the circular functions as sums of exponential functions leads to:

$$A = \frac{b^2}{2} \int_{X_1=0}^{1} [(1-X_1)e^{C_1X_1} + (1-X_1)e^{C_2X_1} + \frac{1}{ir\pi}(e^{C_1X_1} - e^{C_2X_1})]dX_1, \quad \text{(A2-13)}$$

where:

$$\begin{cases} C_1 = -\alpha_x\dfrac{\omega b}{U_c} + ir\pi, \\ C_2 = -\alpha_x\dfrac{\omega b}{U_c} - ir\pi = C_1^*. \end{cases} \quad \text{(A2-14)}$$

Now, a simple expression of A can be obtained, integrating (A2-13) with respect to X_1.
The final result is:

$$A=\frac{b^2}{2}[(\frac{1}{C_1}+\frac{1}{ir\pi})\frac{(e^{C_1}-1)}{C_1}+(\frac{1}{C_1^*}-\frac{1}{ir\pi})\frac{(e^{C_1^*}-1)}{C_1^*}-\frac{2\Re(C_1)}{C_1C_1^*}]. \tag{A2-15}$$

The same kind of calculation can be achieved concerning the B coefficient when $s=n$, and the result is:

$$B=\frac{a^2}{2}\int_{Y_1=0}^{1}[(1-Y_1)e^{C_3Y_1}+(1-Y_1)e^{C_4X_1}+\frac{1}{is\pi}(e^{C_3Y_1}-e^{C_4Y_1})]dY_1, \tag{A2-16}$$

where:

$$\begin{cases} C_3=-\alpha_y\dfrac{\omega a}{U_c}+i(s\pi-\dfrac{\omega a}{U_c}), \\ C_4=-\alpha_y\dfrac{\omega a}{U_c}-i(s\pi+\dfrac{\omega a}{U_c}). \end{cases} \tag{A2-17}$$

An integration permits to obtain the final result for B:

$$B=\frac{a^2}{2}[(\frac{1}{C_3}+\frac{1}{is\pi})\frac{(e^{C_3}-1)}{C_3}+(\frac{1}{C_4}-\frac{1}{is\pi})\frac{(e^{C_4}-1)}{C_4}-\frac{1}{C_3}-\frac{1}{C_4}] \tag{A2-18}$$

*case 2: If $r\neq m$:

An integration of the equation (A2-9) in respect to X_2 leads to:

$$\begin{aligned} A=\frac{b^2}{2}\int_{X_1=-1}^{1}e^{-\alpha_x\left|\frac{\omega bX_1}{U_c}\right|}\Bigg[&\frac{\cos((r+m)\pi\frac{X_1}{2})}{(r-m)\pi}[\sin((r-m)\pi(1-\frac{|X_1|}{2}))-\sin((r-m)\pi\frac{|X_1|}{2})] \\ &+\frac{\sin((r+m)\pi\frac{X_1}{2})}{(r-m)\pi}[\cos((r-m)\pi(1-\frac{|X_1|}{2}))-\cos((r-m)\pi\frac{|X_1|}{2})] \\ &-\frac{\cos((r-m)\pi\frac{X_1}{2})}{(r+m)\pi}[\sin((r+m)\pi(1-\frac{|X_1|}{2}))-\sin((r+m)\pi\frac{|X_1|}{2})] \\ &-\frac{\sin((r-m)\pi\frac{X_1}{2})}{(r+m)\pi}[\cos((r+m)\pi(1-\frac{|X_1|}{2}))-\cos((r+m)\pi\frac{|X_1|}{2})]\Bigg]dX_1. \end{aligned} \tag{A2-19}$$

Assuming that:

$$\begin{cases} E = \dfrac{(r+m)\pi}{2}, \\ F = \dfrac{(r-m)\pi}{2}, \end{cases} \tag{A2-20}$$

we can write the A coefficient as:

$$A = \frac{b^2}{2}\int_{X_1=-1}^{1} e^{-\alpha_x\left|\frac{\omega b X_1}{U_c}\right|}\left[\frac{((-1)^{r+m+1}-1)}{2}\left[\frac{\cos(E\,X_1)}{F}\sin(F|X_1|) - \frac{\cos(F\,X_1)}{E}\sin(E|X_1|)\right]\right. \\ \left. + ((-1)^{r+m}-1)\left[\frac{\sin(E\,X_1)}{F}\cos(F|X_1|) - \frac{\sin(F\,X_1)}{E}\cos(E|X_1|)\right]\right] dX_1. \tag{A2-21}$$

Following the same scheme than in the previous case, it is possible to calculate the exact value of A. The result is:

$$A = \frac{((-1)^{r+m+1}-1)b^2}{2i(r^2-m^2)}\left[m\left(\frac{1}{C_1}(e^{C_1}-1) - \frac{1}{C_1^*}(e^{C_1^*}-1)\right) - r\left(\frac{1}{C_2}(e^{C_2}-1) - \frac{1}{C_2^*}(e^{C_2^*}-1)\right)\right], \tag{A2-22}$$

where:

$$\begin{cases} C_1 = -\alpha_x\dfrac{\omega\, b}{U_c} + ir\pi, \\ C_2 = -\alpha_x\dfrac{\omega\, b}{U_c} + im\pi. \end{cases} \tag{A2-23}$$

Concerning the expression of B, in the $n \neq s$ case, the next result is obtained:

$$B = \frac{((-1)^{s+n+1}-1)a^2}{2i(s^2-n^2)}\left[n\left(\frac{1}{C_1}(e^{C_1}-1) - \frac{1}{C_4}(e^{C_4}-1)\right) - s\left(\frac{1}{C_2}(e^{C_2}-1) - \frac{1}{C_3}(e^{C_3}-1)\right)\right]. \tag{A2-24}$$

Annexe 3: Figures

A-3-a- Figures of radiation efficiency coefficients:

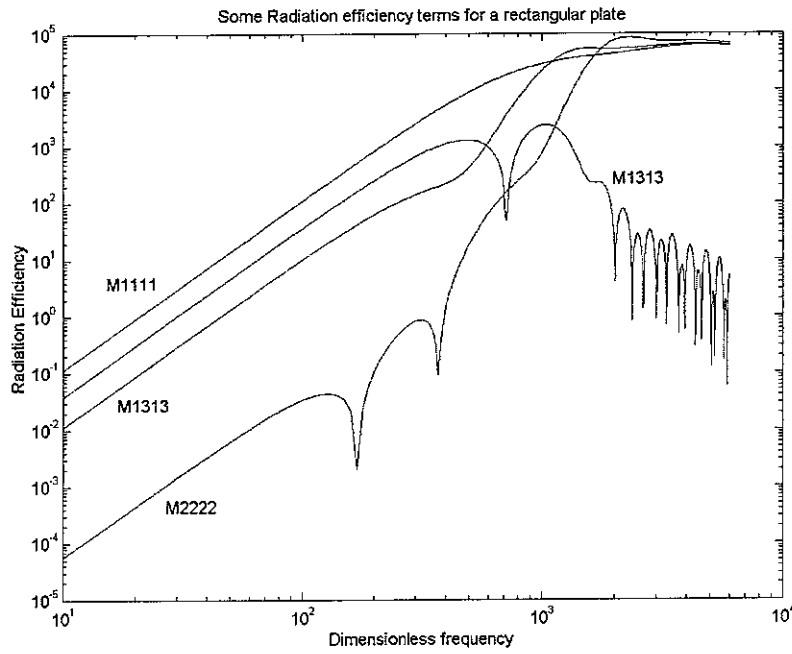

A-3-b1- The total sound power radiated by the G. Gibbs panel:

This figure was obtained with a panel of the same dimension as the one used by G. Gibbs.

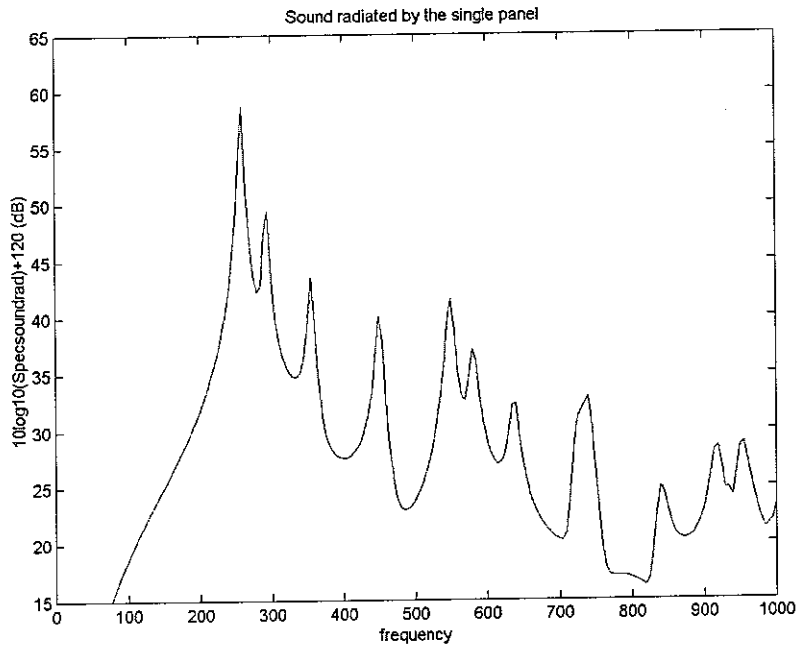

A-3-b2- G. Gibbs measurement of the total sound radiated by the panel:

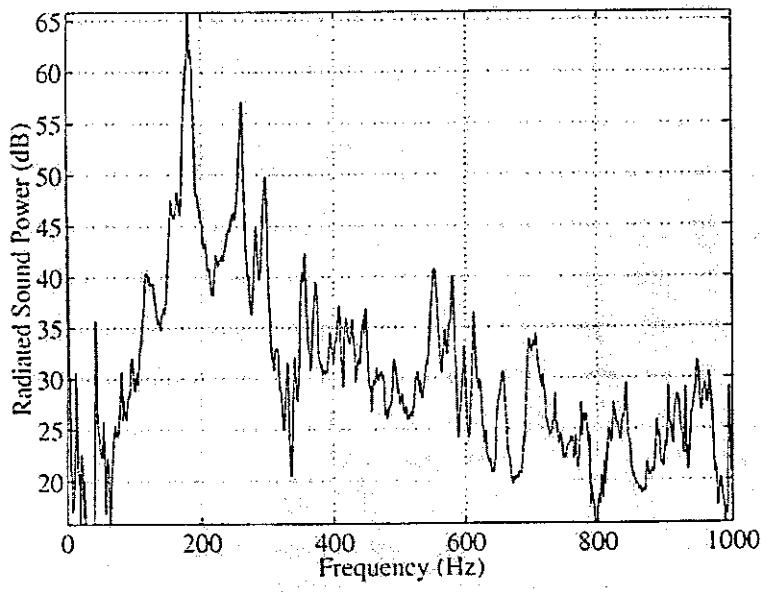

Figure 7 Open Loop Radiated Sound Power at Mach 0.1 (dB re. 1E-12 W)

A-3-c- Figure of the total sound radiated by a panel with the diagonal approximation:

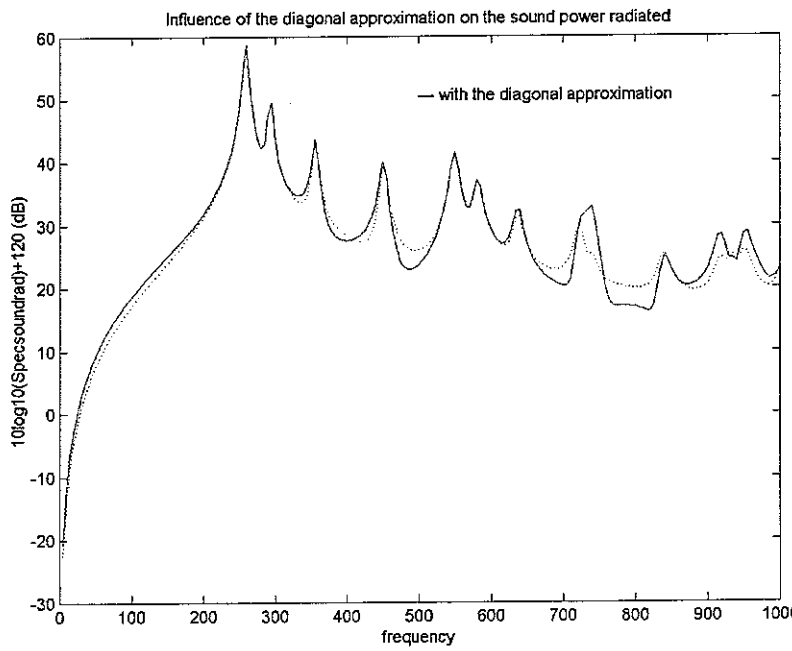

A-3-d1- Influence of the first radiation mode on the volume velocity of the panel:

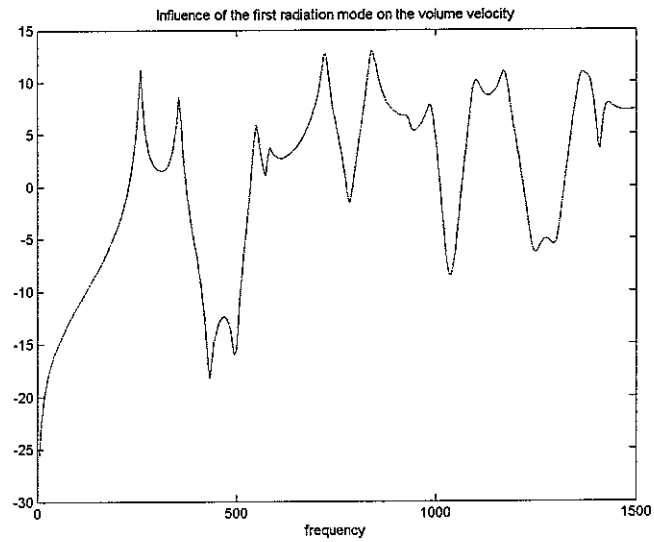

A-3-d2- G. Gibbs measurement of the volume velocity due to the first radiation mode:

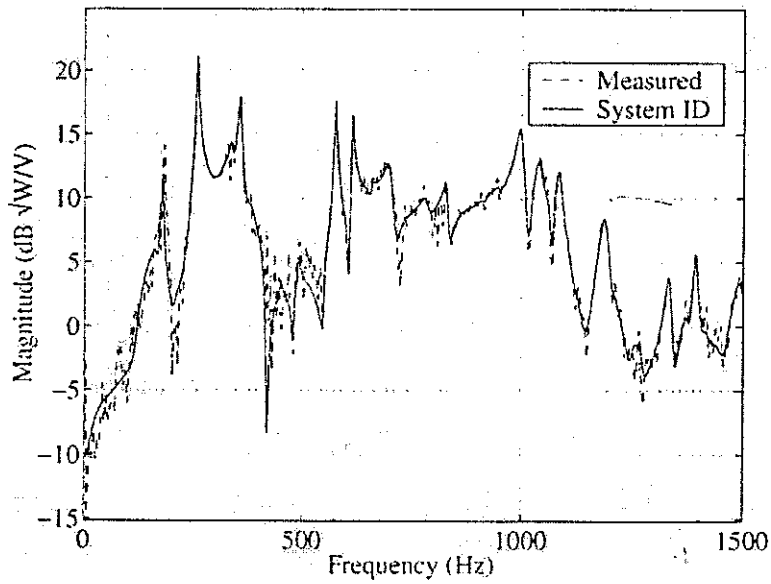

A-3-d3- Phase of the actuator / panel transfer function:

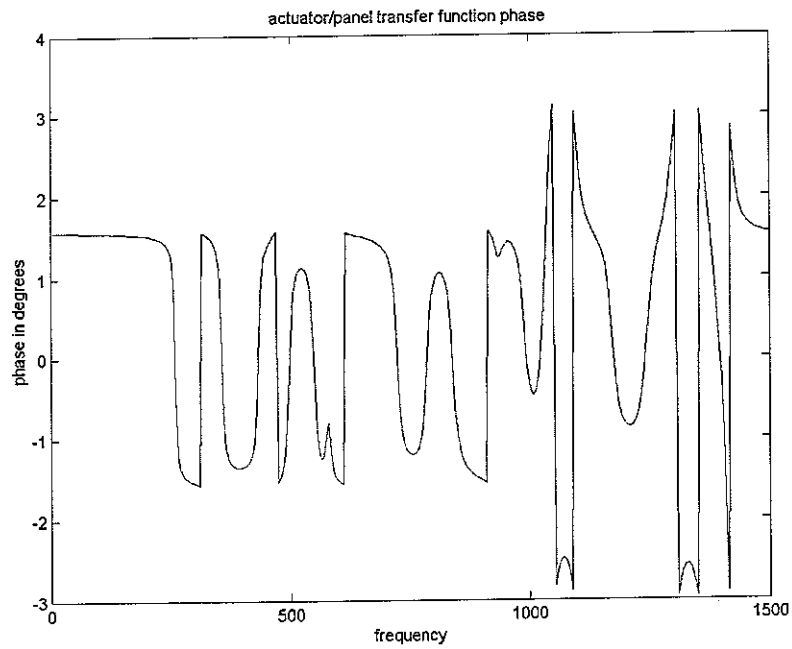

Annexe 4: Calculation of the optimal value of the control filter

The aim of this annexe is to calculate the optimal value of W that minimize the cost function J:

$$J = S_{\pi^-}^2 + \beta W^T W$$

The expression of W is given by:

$$S_{\pi^-} = \frac{\omega \rho c}{2} Tr\left\{diag(A)^H \Re(diag[M])diag(A)diag(\Psi)\right\}$$

For convenience, the *diag* expression will be omited.

Then, the value of the cost function is:

$$J = \Psi' AA'(1 - H_s' W' H_{act}' AA') M' M(1 - AA' H_{act} W H_s) AA'\Psi + \beta W^T W$$

This can be written:

$$\begin{aligned} J = {} & \Psi' AA' M' MAA'\Psi - \Psi' AA' H_s' W' H_{act}' AA' M' MAA'\Psi \ldots \\ & \ldots - \Psi' AA' M' MAA' H_{act} W H_s AA'\Psi \ldots \\ & \ldots + \Psi' AA' H_s' W' H_{act}' AA' M' MAA' H_{act} W H_s AA'\Psi + \beta W^T W \end{aligned}$$

The derivation of such an expression leads to:

$$\begin{aligned} \frac{\partial J}{\partial W} = {} & -H_{act}' AA' M' MAA'\Psi\Psi' AA' H_s' - H_{act}' AA' M' MAA'\Psi\Psi' AA' H_s' + \ldots \\ & \ldots 2H_s AA'\Psi\Psi' AA' H_s' H_{act}' AA' M' MAA' H_{act} W + 2\beta W \end{aligned}$$

J is a quadratic form, so the value of W that minimize it is the one that sets up $\frac{\partial J}{\partial W}$ to zero. This optimal value is then:

$$W_{opt}' = \frac{1}{AA' H_{act} H_s + \dfrac{\beta}{H_{act}' AA' M' MAA'\Psi\Psi' AA' H_s'}}$$